# Spectral Reflectivity and Emissivity Measurements of Solid and Liquid UO$_2$ at 458, 514.5 and 647 nm as a Function of Polarization and Angle of Incidence

M. Bober, J. Singer, K. Wagner
Institut für Neutronenphysik und Reaktortechnik
Projekt Schneller Brüter

Kernforschungszentrum Karlsruhe

KERNFORSCHUNGSZENTRUM KARLSRUHE

Institut für Neutronenphysik und Reaktortechnik
Projekt Schneller Brüter

KfK 3023

Spectral Reflectivity and Emissivity Measurements of
Solid and Liquid $UO_2$ at 458, 514.5 and 647 nm as a
Function of Polarization and Angle of Incidence

M. Bober, J. Singer, K. Wagner

Kernforschungszentrum Karlsruhe GmbH, Karlsruhe

# Abstract

The directional spectral reflectivity of $UO_2$ was measured in the temperature range between 2000 and 4000 K with an integrating-sphere laser reflectometer. The measurements were carried out with monochromatic light polarized parallel and perpendicular, respectively, to the plane of incidence at the three wavelengths of 458, 514.5 and 647 nm, and at the angles of incidence of 35, 45 and 72$^{\circ}$. The reflectivity shows a slight decrease with increasing wavelength and a distinct decrease with increasing temperature above the melting point. The directional emissivity is related to the reflectivity by Kirchhoff's law. An evaluation of the hemispherical emissivity yielded values by 5% lower than the near-normal directional emissivity. From the reflectivity measured vs. the angle of incidence and the polarization, the optical constants n, k of liquid $UO_2$ were computed. Preliminary values of n=2.0 and k=0.6 were obtained for the temperature range between 3000 and 3500 K at the wavelength of 514.5 nm. The value of k=0.6 corresponds to a penetration depth of radiation of about 0.1 $\mu$m in $UO_2$. An estimation shows that internal radiative heat transfer cannot cause a significant increase of the thermal conductivity of liquid $UO_2$.

Messungen des spektralen Reflexions- und Emissionsgrades von
festem und flüssigem $UO_2$ bei 458, 514,5 und 647 nm als Funktion
der Polarisation und des Einfallswinkels

Zusammenfassung

Der gerichtete spektrale Reflexionsgrad von $UO_2$ wurde im Tempera-
turbereich zwischen 2000 K und 4000 K mit einem integrierenden
Laser-Kugelreflektometer gemessen. Die Messungen wurden sowohl
mit parallel als auch mit senkrecht zur Einfallsebene polarisier-
tem monochromatischem Licht bei den Wellenlängen 458, 514,5 und
647 nm und den Reflexionswinkeln von 35,45 und 72$^{\circ}$ durchgeführt.
Der resultierende Reflexionsgrad von $UO_2$ erweist sich nur schwach
wellenlängenabhängig. Er wird mit wachsender Wellenlänge geringfügig
kleiner und nimmt mit zunehmender Temperatur oberhalb des Schmelz-
punktes deutlich ab.


Aus dem spektralen Reflexionsgrad läßt sich mit Hilfe des Kirch-
hoff'schen Gesetzes der spektrale Emissionsgrad errechnen. Die
Berechnung des halbräumlichen Emissionsgrades aus der gemessenen
Winkelabhängigkeit des gerichteten Emissionsgrades führt zu Werten
die 5% kleiner sind als die des gerichteten Emissionsgrades bei
nahezu  senkrechter Emission. Aus dem in Abhängigkeit vom Einfalls-
winkel und von der Polarisation gemessenen Reflexionsgrad lassen
sich die optischen Konstanten n und k für flüssiges $UO_2$ berechnen.
Erste Auswertungen bei der Wellenlänge 514,5 nm liefern für den
Temperaturbereich zwischen 3000 K und 3500 K die Werte n=2,0 und
k=0,6. Dem Wert k=0,6 entspricht eine Eindringtiefe der Strahlung
in $UO_2$ von etwa 0,1 µm. Eine Abschätzung zeigt, daß innerer Strah-
lungswärmetransport nicht wesentlich zu einem Anstieg der Wärme-
leitfähigkeit von flüssigem $UO_2$ beitragen kann.

# 1. Introduction

The safety analysis of nuclear reactors requires knowledge of the thermal radiation properties of the nuclear fuel materials at high temperatures. In order to make accurrate radiative transfer calculations, the spectral emittance and the optical constants of the fuel must be known up to temperatures well in excess of its melting point. The spectral emittance determines the radiative heat transfer from the fuel to adjacent vapor spaces, while the optical constants determine the radiative heat transfer in the condensed phase. The latter contributes to the thermal conductivity of the fuel. Besides, information on the optical constants could help to determine the unknown physical structure of the liquid fuel and its chemical bonding character. The knowledge of the spectral emissivity also allows reliable pyrometric measurements of the temperature of fuel melts to be made in high-temperature experiments.

Referring to thermal diffusivity measurements with liquid $UO_2$ /1/ a significant increase in the thermal conductivity is assumed for $UO_2$ upon melting. This could be attributed to electronic and radiative contributions respectively. To estimate the possible amount of the radiative contribution, the spectral course of the absorption coefficient has to be taken into account from the infrared to the visible wavelengths. However, the only data available for $UO_2$ are the low temperature values of the refractive index determined in the visible range /2/ and of the spectral absorption coefficient measured from the near infrared down to the absorption edge in the visible red /3-5/. No experimental data exist for molten $UO_2$. Previous theoretical studies on the contribution of the internal radiative heat transfer to the thermal conductivity of $UO_2$ have been based on the lower temperature absorption data for single crystal $UO_2$ extrapolated in the liquid state /5-7/. Up to now the question has not been answered definitely whether electronic or radiative thermal transport is dominant in liquid $UO_2$. For reliable calculations of the radiative transfer in molten $UO_2$ there is an urgent need of high temperature spectral absorption data in particular at wavelengths in the visible range.

Only a few measurements of the spectral reflectance and emittance of $UO_2$ were reported. The reflectivity of single crystal $UO_2$ was determined by Schoenes /8/ in a wide spectral range at room temperature. Spectral emissivities of sintered $UO_2$ measured in the infrared and visible red at temperatures up to 2400 K were published by Cabannes et al /9/ and by Held and Wilder /10/. Recently, we measured the normal spectral reflectivity and emissivity of molten $UO_2$ up to temperatures of 4000 K at the wavelengths of 0.63 and 10.6 µm /11/. All experimental results reported indicate that the emittance of sintered $UO_2$ does not appreciably depend on the temperature, surface roughness, density, or stoichiometric deviations. The emissivity of liquid $UO_2$ measured at 0.63 µm shows a distinct increase with temperature, whereas at 10.6 µm it decreases with increasing temperature. The measured reflectivity of the refrozen sample surface shows good agreement with Schoenes' results obtained with single crystal $UO_2$.

Our reflectance measurements on molten $UO_2$ were made with an integrating sphere reflectometer in which laser beam heating of the sample material is used. These measurements have been continued and extended to various wavelengths in the visible spectral range. The dependence of the reflectivity of the heated sample on the angle of incidence and the polarization of the incident light have been included in the investigation. It has been an objective of these measurements to estimate the total thermal emittance of the liquid material and to evaluate approximately its optical constants. Preliminary results for liquid $UO_2$ have been reported /12/.

## 2. Basic relations for the measurements

Reflectance measurements performed with polarized monochromatic radiation, particularly with non-normal incidence, allow both to determine the spectral emissivity of the sample surface and to evaluate the optical constants of the bulk material provided that the specimen surface is optically smooth. Precise values of the spectral emittance can be obtained from reflectance measurements if the transmittance of the sample considered approaches zero. This applies to the thickness of the surface layer of $UO_2$ heated up quasi-isothermally in the laser reflectometer /13/.

The spectral directional emittance $\varepsilon_{\lambda,T}(\theta)$ of the flat specimen surface irradiated from the desired direction is related to the directional-hemispherical reflectance $\rho_{\lambda,T}(\theta;2\pi)$ by Kirchhoff's law,

$$\varepsilon_{\lambda,T}(\theta) = 1 - \rho_{\lambda,T}(\theta;2\pi). \tag{1}$$

If the surface is smooth so that only specular reflection occurs, the directional emissivity equals 1 minus the specular reflectivity $\rho_{\lambda,T}(\theta)$ in that direction.

With the values of the spectral directional emittance measured at various angles of incidence the hemispherical emittance $\varepsilon_{\lambda,T}^{h}$ is obtained by integrating the directional emittance over the hemispherical space. Assuming that an azimuthal dependence of the emittance does not exist, we obtain

$$\varepsilon_{\lambda,T}^{h} = 2 \int_{0}^{1} \varepsilon_{\lambda,T}(t) \cdot t \cdot dt; \qquad t=\cos\theta. \tag{2}$$

For a given wavelength interval $(\lambda_1,\lambda_2)$ an average value of the emittance can be defined as

$$\varepsilon_{\Delta\lambda,T} = \int_{\lambda_1}^{\lambda_2} \varepsilon_{\lambda,T} \cdot I_{\lambda,T} d\lambda \Big/ \int_{\lambda_1}^{\lambda_2} I_{\lambda,T} d\lambda \tag{3}$$

where $I_{\lambda,T}$ is the Planck black body radiation function, and $\varepsilon_{\lambda,T}$ is the directional or hemispherical emittance, respectively.

The optical constants, i.e. the refractive index n and the absorption coefficient k, are the real and imaginary parts of the complex index of refraction of the absorbing material:

$$N_{\lambda,T} = n - ik.$$

Both n and k are functions of the temperature and the wavelength. The absorption coefficient is related to the absorption constant $\alpha_{\lambda,T}$, as measured by the transmission method, by the equation

$$\alpha_{\lambda,T} = 4\pi k/\lambda. \tag{4}$$

The reciprocal of $\alpha_{\lambda,T}$ is the penetration depth of radiation in the material. This is the characteristic quantity which enters in a spectrally averaged form the expression for the radiative thermal conductivity in the optically thick limit approximation (see for example Özisik /14/).

The optical constants can be found by analysing the state of elliptical polarization which appears when plane polarized radiation is reflected obliquely from an optically smooth surface or by evaluating the respective variation of the polarized components of reflected energy with the angle of incidence. Various measuring methods are described in the literature indicated in the review by Shestakov et al /15/. The most suitable parameters to measure are the reflectances $\rho_s$ and $\rho_p$ for the incident radiation polarized perpendicular and parallel, respectively, to the plane of incidence, the intensity ratio of $\rho_s$ and $\rho_p$, and the relative phase difference.

One method introduced by Avery /16/ is based on the measurement of the intensity ratio of $\rho_p$ and $\rho_s$ for at least two different angles of incidence. This method is assumed to be appropriate for evaluation of the reflectivity measurements performed on molten $UO_2$ in an integrating sphere reflectometer since it is based solely on energy measurements without regard of phase relations /17/. By measuring the ratio $\rho_p/\rho_s$ the accuracy of the experiments is improved as this ratio varies more rapidly with the angle of incidence than $\rho_p$ and $\rho_s$ alone and because, in principle, absolute reflectance measurements are not necessary. In order to get sufficiently sensitive to the amounts of n and k, Avery's method requires a suitable choice of the measurement angles /18/. The angles of incidence should be chosen such that one is just below and one just above the principle angle of incidence at which $\rho_p$ and $\rho_s$ differ in phase by $90^\circ$. This angle is near the angle where $\rho_p/\rho_s$ is minimum.

Based on the generalized Fresnel reflection equations, mathematical expressions of the reflectivity components are obtained for the perpendicular and parallel polarizations, respectively, which are related to the optical constants and to the angle of incidence $\theta$ (see, for example, Born and Wolf /19/):

$$\rho_s(\theta) = \frac{(a - \cos\theta)^2 + b^2}{(a + \cos\theta)^2 + b^2} \, , \tag{5}$$

$$\rho_p(\theta) = \rho_s(\theta) \frac{(a - \sin\theta \, \tan\theta)^2 + b^2}{(a + \sin\theta \, \tan\theta)^2 + b^2} \tag{6}$$

where

$$a^2 = 0.5 \left[ (n^2-k^2-\sin^2\theta) + \sqrt{(n^2-k^2-\sin^2\theta)^2 + 4n^2k^2} \right]$$

$$b^2 = 0.5 \left[ -(n^2-k^2-\sin^2\theta) + \sqrt{(n^2-k^2-\sin^2\theta)^2 + 4n^2k^2} \right] .$$

The principal angle of incidence $\theta_o$ is related to n and k by /20/

$$(n^2+k^2)^2 - 2(n^2-k^2)\sin^2\theta_o = (\tan^4\theta_o - 1) \sin^4\theta_o. \tag{7}$$

There is a useful relation between $\rho_s$ and $\rho_p$ for the angle of incidence $\theta=45^\circ$ which allows to check experimental data:

$$\rho_s^2 = \rho_p . \tag{8}$$

For normally impinging radiation there is no preferred plane of incidence and $\rho(0) = \rho_s = \rho_p$. From equation (5) follows the familar relation:

$$\rho(0) = \frac{(n-1)^2 + k^2}{(n+1)^2 + k^2} . \tag{9}$$

With measured values of $\rho_s$ and $\rho_p$, the reflectance $\rho(\theta)$ of the natural or unpolarized radiation can easily be obtained for each angle $\theta$. $\rho(\theta)$ is defined by

$$\rho(\theta) = 0.5 \ (\rho_s(\theta) + \rho_p(\theta)). \tag{10}$$

## 3. Measuring method

For measurement of the spectral reflectance of liquid ceramic materials, an integrating-sphere laser reflectometer was developed which operates on laser-beam heating. The experimental set-up has been described in detail elsewhere /13,21/.

Figure 1 shows schematically the principle of the measuring method. A small specimen is located in an integrating sphere of 200 mm diameter. With a focused $CO_2$ laser beam of 500 W power the surface of the specimen is heated for millisecond intervals to temperatures between 3000 and 4000 K. The size of the heated surface area, 0.5 to 0.6 mm in diameter, depends on the temperature and heating rate which can be varied by variation of the $CO_2$-laser power density. Parallel with heating, the center of the heated surface area is irradiated by the light beam of a reference laser set at the measurement wavelength $\lambda$. The reflected portion of the reference light is isotropically scattered by the diffuse-reflective integrating sphere and measured with a spectral photomultiplier detector placed at a small aperture in the sphere wall.

Placing a spectral line filter of the wavelength $\lambda$ in front of the detector together with high-frequency modulation of the incident reference light allows to detect the reflected light in the presence of the thermal radiation background emitted from the heated sample. The demodulated reflection signal then yields the reflectance of the sample by means of an additional calibration measurement where the specimen is replaced by a perfectly reflecting mirror of the same size. From equation (1) the corresponding emittance of the sample is obtained.
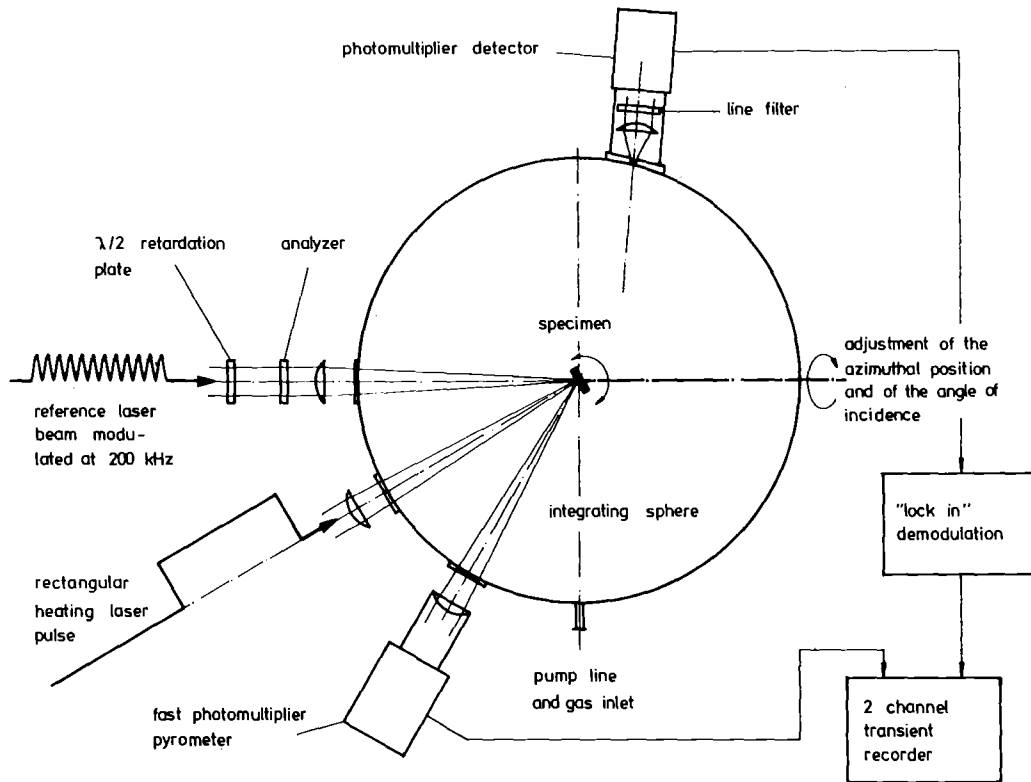
Figure 1:  Principle of the measuring method

The surface temperature of the heated sample is determined by
means of a fast micropyrometer working at the wavelength of
633 nm at which the spectral emittance of liquid $UO_2$ is known
as a function of the radiance temperature /22/. During the reflec-
tion measurements a pure inert gas atmosphere is maintained in the
sphere at $\sim$2 bar pressure level to suppress surface evaporation of
the sample. The angle of incidence $\theta$ can be set between 5 and 75°
by altering the inclination of the sample. By use of a half-wave
retarder of the wavelength $\lambda$ together with an analyser, the plane
of polarization of the incident reference light is precisely
adjusted with respect to the plane of incidence. Reference light
sources are Kr-ion and Ar-ion lasers of some 100 mW power modulated
at 200 kHz, which allow measurements at about 10 wavelengths in the
visible range between 400 and 750 nm.

## 4. Measurements and results

The specimen material used was nuclear-reactor grade, stoichio-
metric $UO_2$ sintered to 96% of the theoretical density with resi-
dual impurities of less than 100 ppm C and 200 ppm Si + Cr + Fe.
For the reflectance measurements, polished disks were prepared
which were 6 mm in diameter and 1 mm thick. Some additional ex-
periments were made with single crystalline material. Smooth
surfaced samples were generated by degassing and liquefying the
surface layer of the specimens, applying surface heating with the
$CO_2$ laser beam immediately before measurements.

Reflectance measurements have been carried out on liquid and re-
frozen sample surfaces in the temperature range between 2000 and
4000 K at the three wavelengths of 647, 514.5 and 458 nm, and at
angles of incidence of 35, 45 and 72°. Figure 2 shows examples
of oscilloscope recordings of reflectivity signals and pyrometer
signals measured on $UO_2$. The plateau in the pyrometer signal which
follows the steep temperature decrease indicates the freezing point.
The reflectivity signals reveal a decrease of reflectivity with
increasing temperature above the melting point.
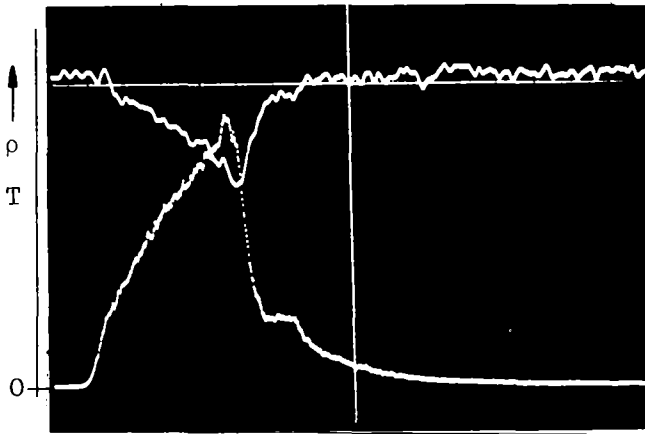
$\theta = 17^{O}$, $\lambda = 647$ nm, $T_{max}=3780$ K
$\rho_{s}$ : 0,035 units/cm
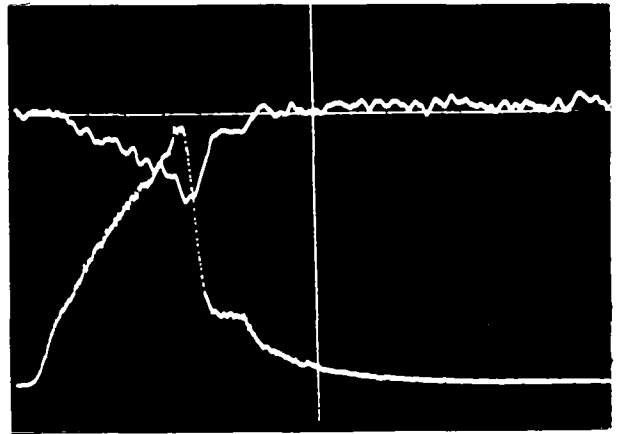
$\theta = 17^{O}$, $\lambda = 647$ nm, $T_{max}=3760$ K
$\rho_{p}$: 0,035 units/cm
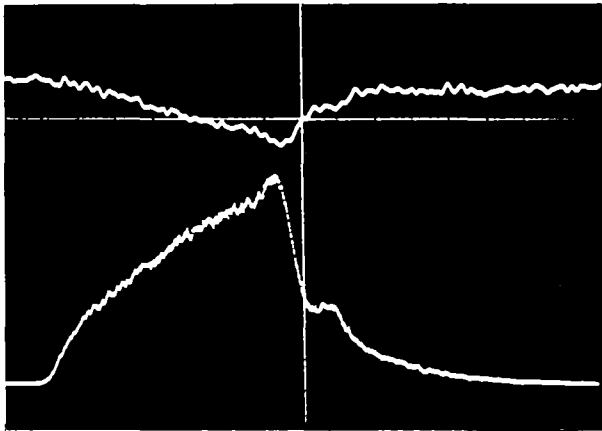
$\theta = 45^{O}$, $\lambda= 458$ nm, $T_{max}=3780$ K
$\rho_{s}$ : 0,075 units/cm
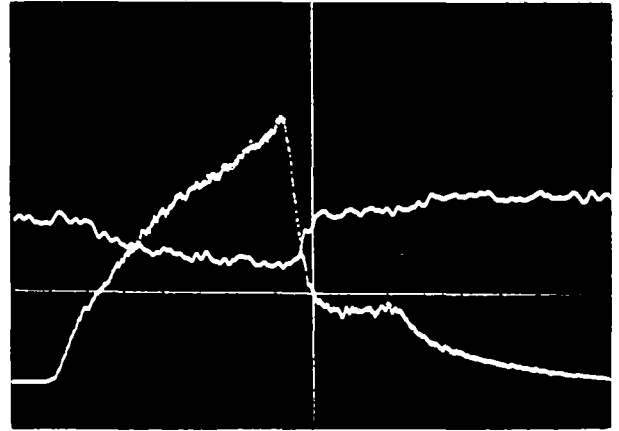
$\theta = 45^{O}$, $\lambda = 514,5$ nm, $T_{max}=3700$ K
$\rho_{p}$: 0,035 units/cm
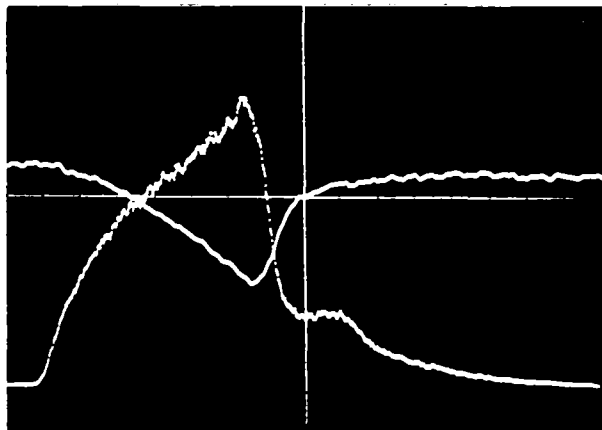
$\theta = 72^{O}$, $\lambda = 514,5$ nm, $T_{max}=3770$ K
$\rho_{s}$ : 0,20 units/cm
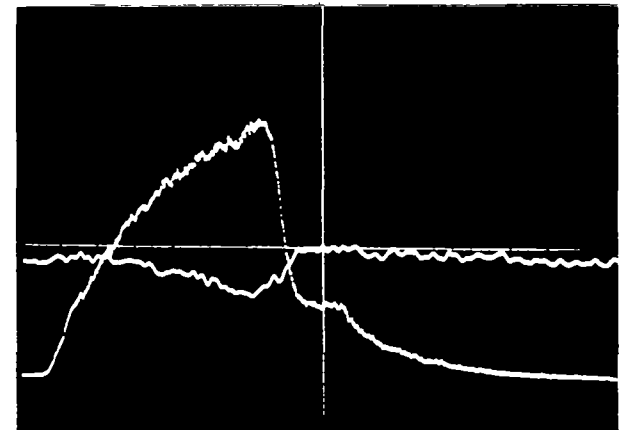
$\theta = 72^{O}$, $\lambda = 458$ nm, $T_{max}=3700$ K
$\rho_{p}$ : 0,035 units/cm

Figure 2: Digital oscilloscope recordings of reflectivity signals (upper trace) and pyrometer signals (lower trace) measured on $UO_2$ at three wavelengths $\lambda$ and various angles of incidence $\theta$, sweep time 5 ms.

About 25 series of measurements have been evaluated for each
wavelength and each angle of incidence. The resulting reflecti-
vities obtained for the polarized components $\rho_s$ and $\rho_p$ (polarized
perpendicular and parallel to the plane of incidence, respectively)
are shown in tables 1a-i and figures 3a-i as a function of the
temperature. Tables are given in the Appendix. The scattering of
the experimental values indicated in figures 3a-i by the circles
and cross marks along the average curves of $\rho_s$ and $\rho_p$, respective-
ly, represents the range of uncertainty of the single measurements.
The reflectivity curves for the unpolarized radiation $\rho$ have been
obtained from $\rho_s$ and $\rho_p$ with equation (10). Tables 2a-c give values
for $\rho_s$, $\rho_p$, $\rho_p/\rho_s$, and $\rho$ averaged at different temperatures for the
three wavelengths and angles of incidence. The results of the
additional measurements on single crystal material are in agreement
with those obtained for the premolten, sintered material(cf. table 1b).
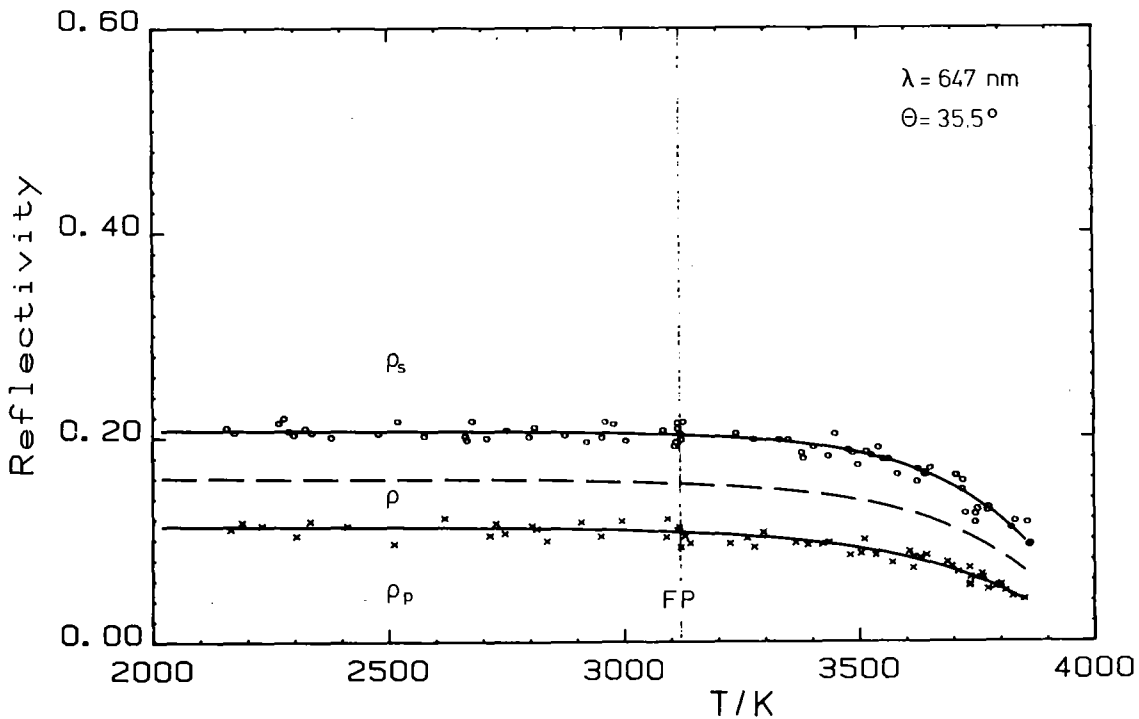


Figure 3a: Spectral directional reflectivity of $UO_2$ for polarized radiation as
a function of the temperature. $\lambda$=647 nm, $\theta$=35.5°. FP=freezing point.
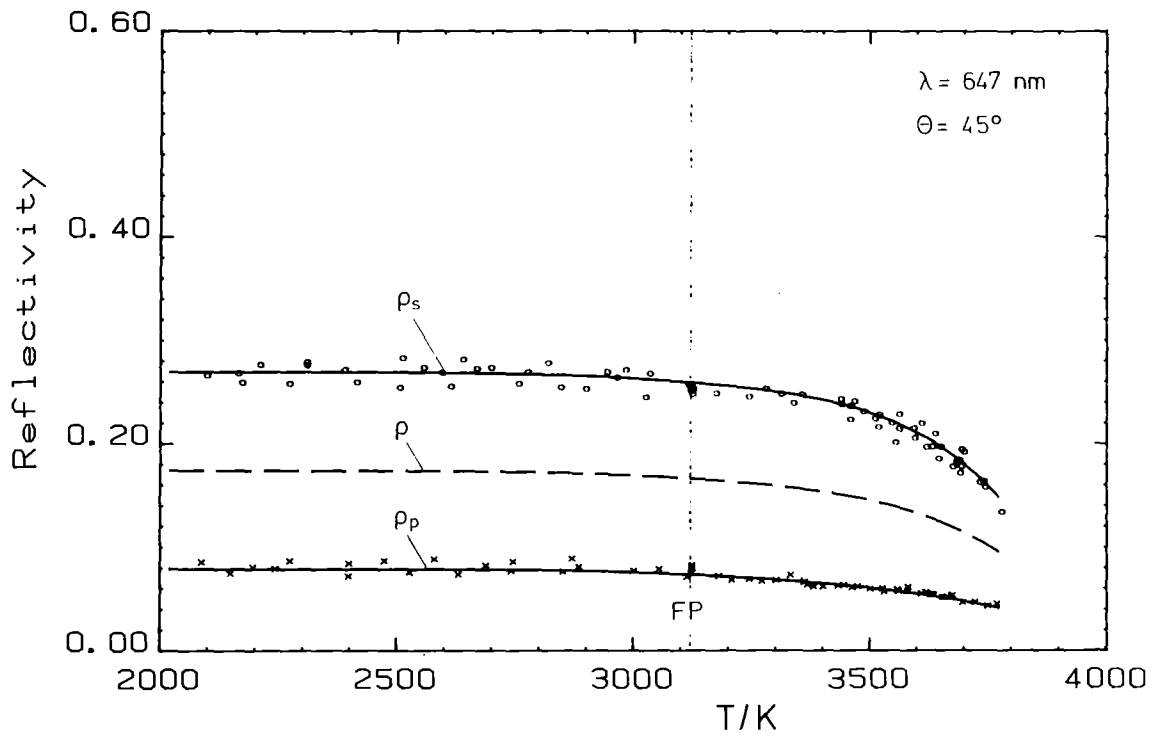
Figure 3b: Spectral directional reflectivity of $UO_2$ for polarized radiation as a function of the temperature. $\lambda$=647nm, $\theta$=45$^\circ$. FP=freezing point.
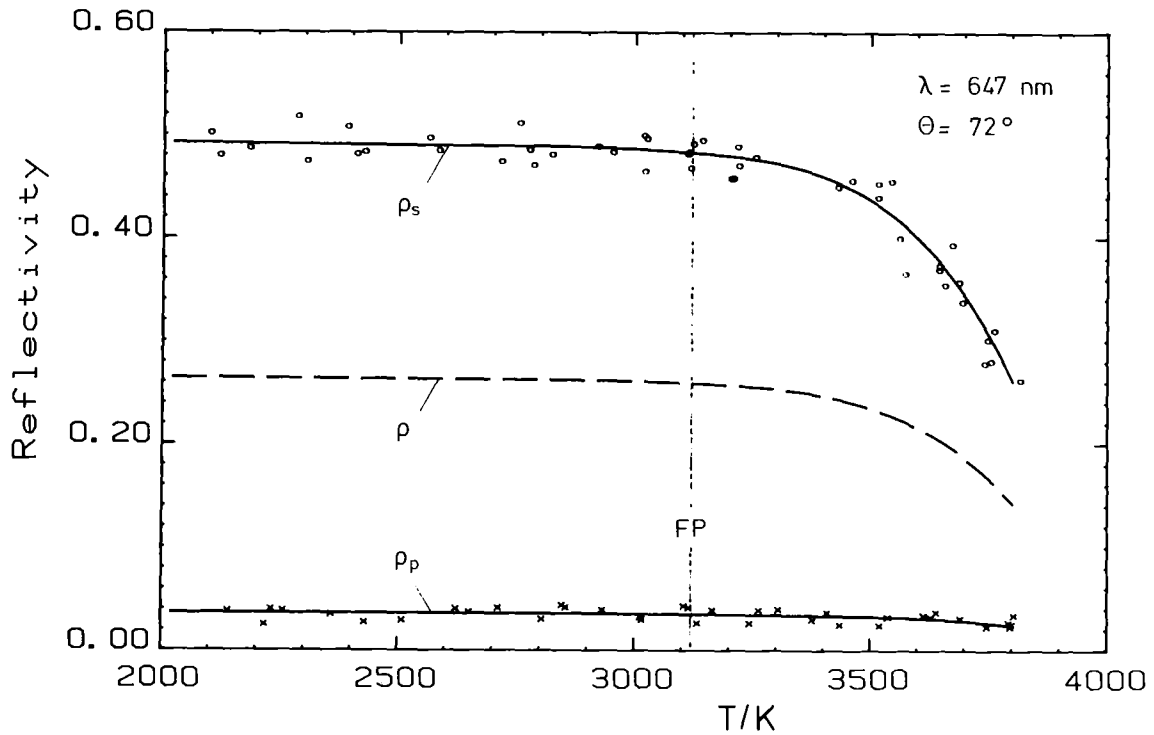


Figure 3c: Spectral directional reflectivity of $UO_2$ for polarized radiation as a function of the temperature. $\lambda$=647nm, $\theta$=72$^\circ$. FP=freezing point.
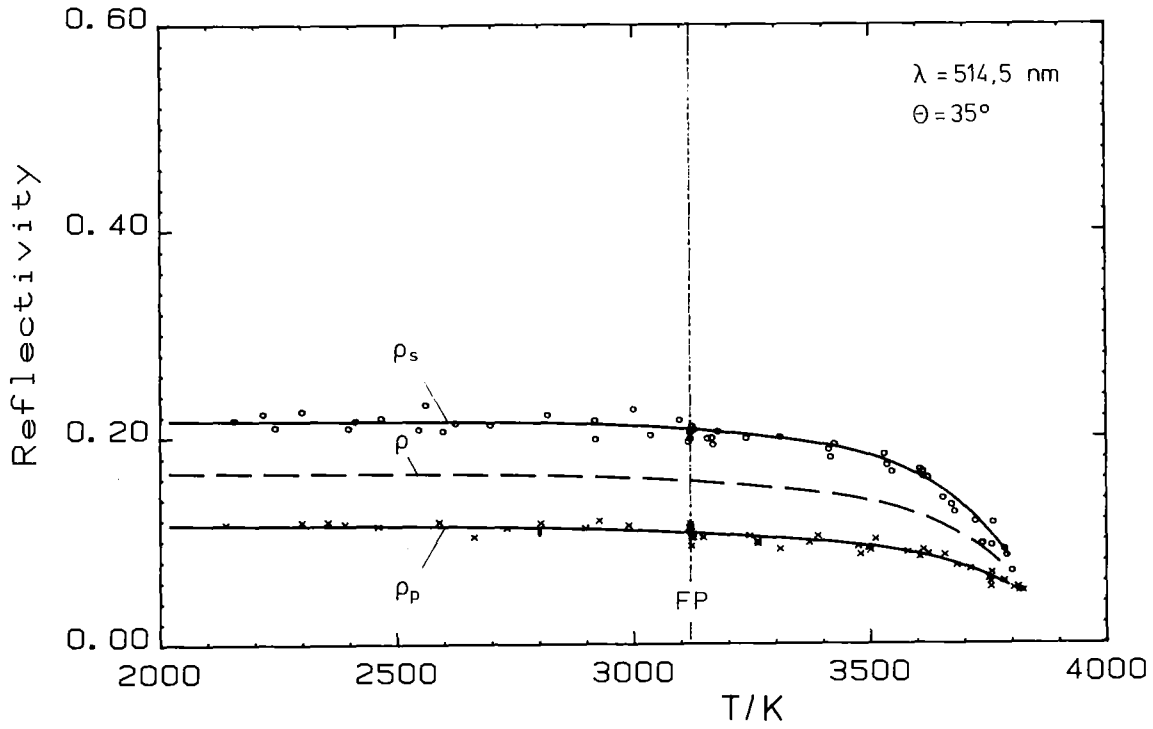
Figure 3d: Spectral directional reflectivity of $UO_2$ for polarized radiation as a function of the temperature. $\lambda$=514.5nm, $\theta$=35°. FP=freezing point
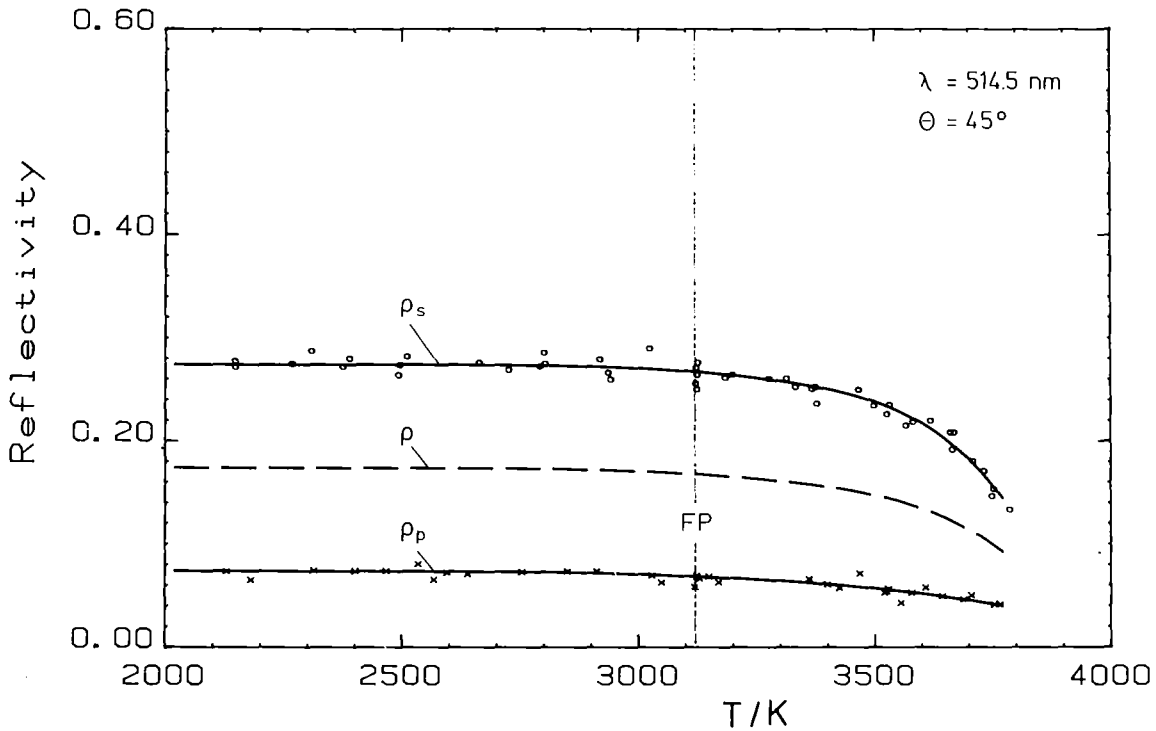


Figure 3e: Spectral directional reflectivity of $UO_2$ for polarized radiation as a function of the temperature. $\lambda$=514.5nm, $\theta$=45°. FP=freezing point.
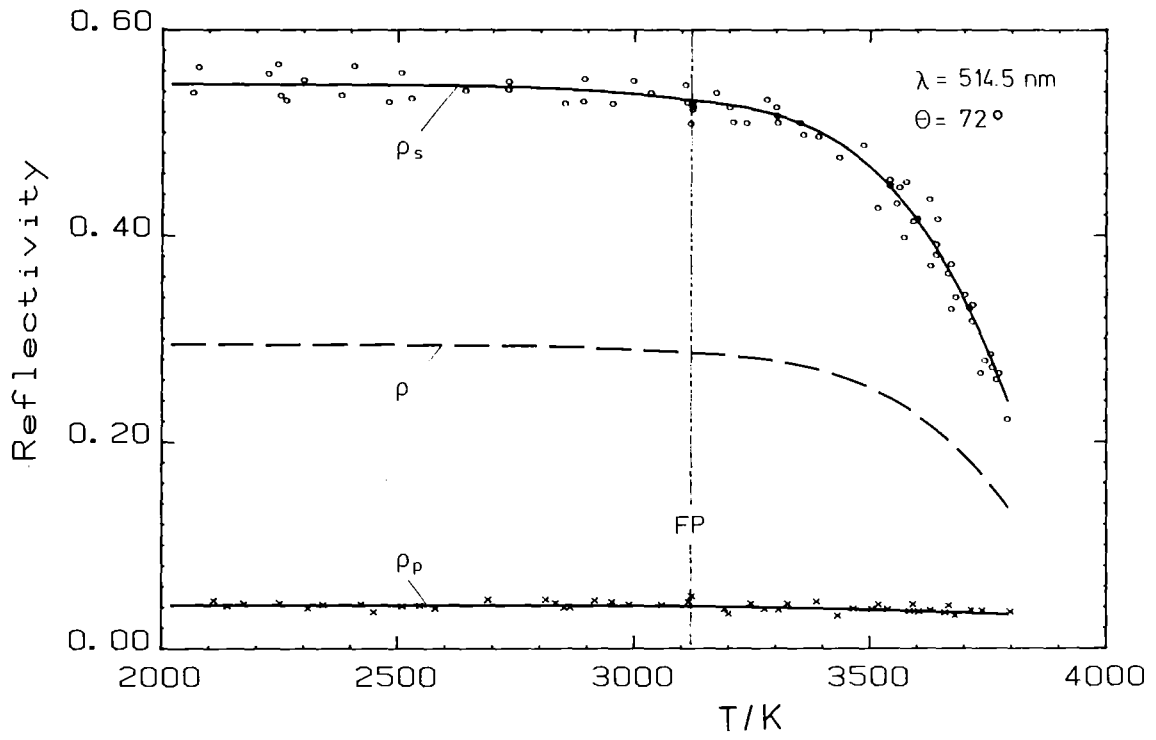
Figure 3f: Spectral directional reflectivity of $UO_2$ for polarized radiation as a function of the temperature. $\lambda=514.5$ nm, $\theta=72°$. FP=freezing point.
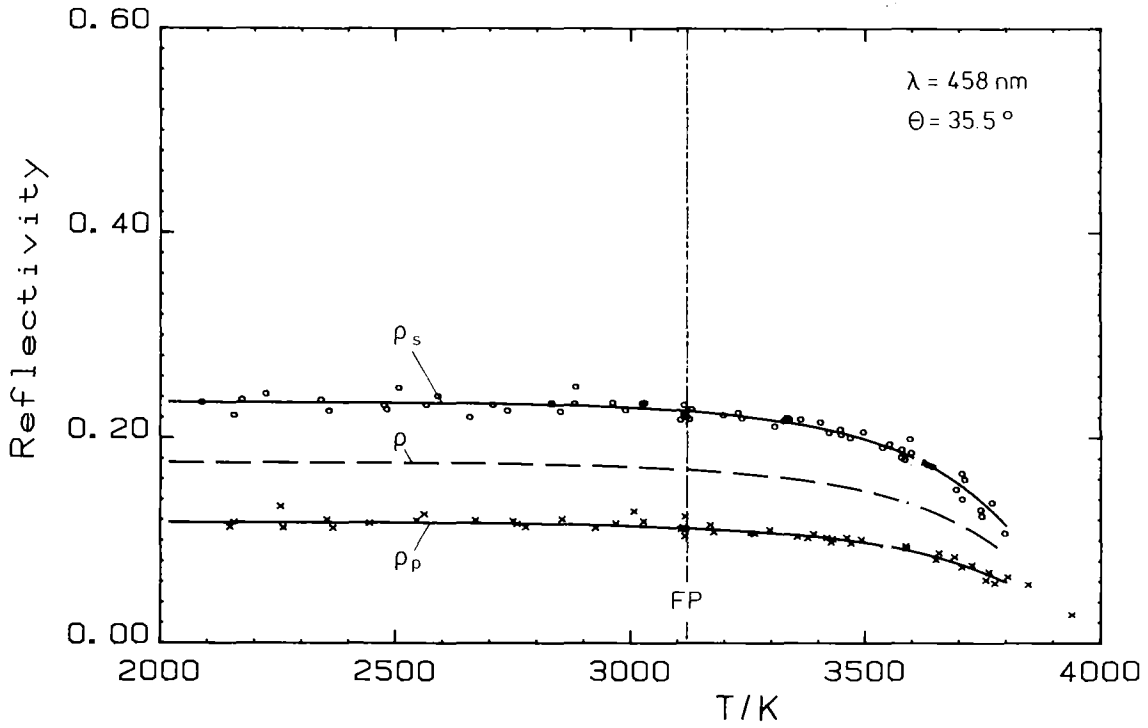
Figure 3g:   Spectral directional reflectivity of $UO_2$ for polarized radiation as a function of the temperature.   $\lambda$=458 nm, $\theta$=35.5°. FP=freezing point.
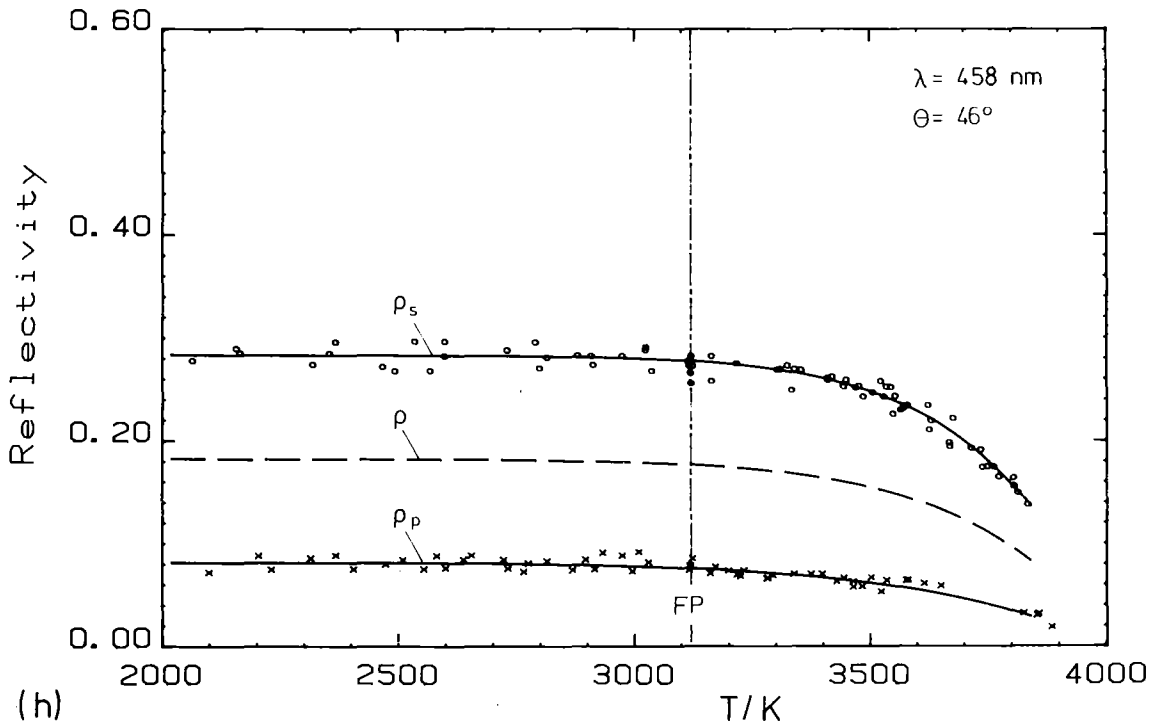


Figure 3h:   Spectral directional reflectivity of $UO_2$ for polarized radiation as a function of the temperature.   $\lambda$=458nm, $\theta$=46°. FP=freezing point.
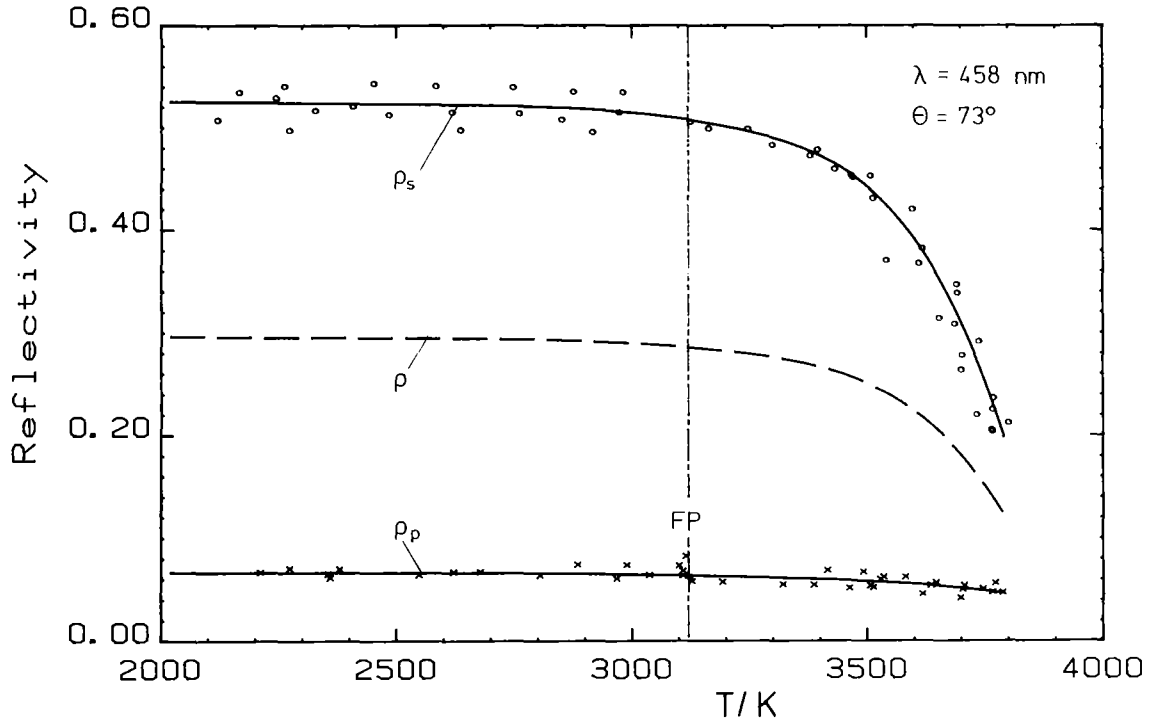
Figure 3i: Spectral directional reflectivity of $UO_2$ for polarized radiation as a function of the temperature. $\lambda$=458 nm, $\theta$=73°. FP=freezing point.

As shown by the diagrams of the figures 3a-i there is little varia-tion of the reflectivity of $UO_2$ with the wavelength in the spectral range considered. Only a slight increase in reflectivity is indi-cated with decreasing wavelength. All reflectance curves show a similar dependence on the temperature. Below the melting point the reflectivity is nearly independent of the temperature, whereas at temperatures above the melting point it clearly decreases with the temperature. Most striking is the variation of the reflectivity for the polarized components with the angle of incidence. In accordance with the Fresnel reflection equations, the reflectivity for the component $\rho_s$ increases with increasing angle of incidence whereas the reflectivity for the component $\rho_p$ decreases. At the angle of incidence of 72°, that's near the principal angle of in-cidence, $\rho_p$ approaches a minimum.

Using the values of the directional spectral emissivity for the unpolarized radiation, which have been determined from the values of $\rho$ with equation (1), and taking into account their angular

dependence, the hemispherical spectral emittance has been estimated from equation (2). The results for the near-normal emissivity $\varepsilon^n$ obtained from the $35^O$ measurements and for the respective hemispherical emittance $\varepsilon^h$ are given in table 3 and figure 4 as a function of the temperature. The bars along the curves shown in figure 4 represent the ranges of uncertainty including both experimental scattering and possible systematic errors. At the three wavelenghts investigated the hemispherical spectral emittance is by about 5% lower than the normal emissivity. The difference decreases slightly with increasing temperature. A similar course is found for the emittance averaged over the wavelength interval $\Delta\lambda$ (458 nm, 647 nm) by means of equation (3) (cf. table 4). Considering the small variation of the spectral emissivity with the wavelength, the averaged emittance can give a hint on the total thermal emittance of liquid $UO_2$, at least for the highest temperatures near 4000 K where the maximum thermal emittance is shifted towards the visible spectral range.

To evaluate the optical constants of $UO_2$, the ratios $\rho_p/\rho_s$ have been determined for several temperatures from the reflectivity curves measured at the angles of incidence of $45^O$ and $72^O$, respectively (cf. tables 2a-c). For each temperature these values have been introduced in equation (6) and the corresponding values of n and k have been computed which satisfy the equation for both ratios $\rho_p/\rho_n$. Results for the temperature range between 3000 and 3500 K are given below.

| T/K | $\lambda$=647 nm | | $\lambda$=514.5 nm | | $\lambda$=458 nm | |
|-----|------|------|------|------|------|------|
|     | n    | k    | n    | k    | n    | k    |
| 3000 | 2.09 | 0.72 | 2.04 | 0.68 | 1.89 | 0.89 |
| 3200 | 2.08 | 0.68 | 2.02 | 0.62 | 1.89 | 0.87 |
| 3500 | 2.03 | 0.61 | 1.98 | 0.58 | 1.84 | 0.80 |

The calculated values indicate only a little temperature dependence of n whereas k shows a tendency to decrease with increasing temperature. Toward the blue spectral range the values of k increase with decreasing wavelength. A discontinuity at the solid-liquid phase transition (3120 K) was not detected.
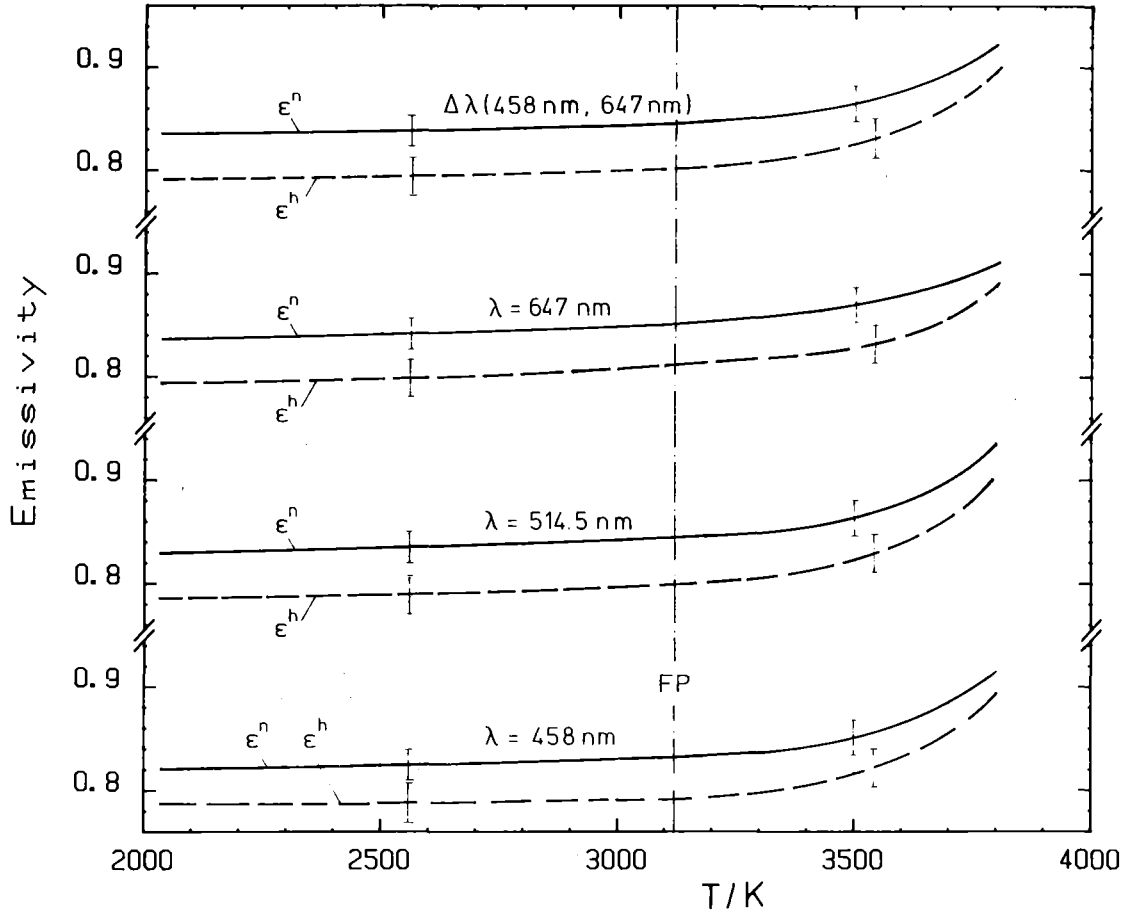
Figure 4: Normal ($\varepsilon^n$) and hemispherical ($\varepsilon^h$) spectral emissivities of $UO_2$ obtained at the wavelengths of 647, 514.5 and 458 nm and in the wavelength interval (458 nm, 647 nm) as a function of the temperature. FP=freezing point.

There are two criteria which give an indication of the
reliability of the values obtained for n and k. Equation (8)
allows to check the accuracy of $\rho_s$ and $\rho_p$ measured at $\theta=45°$.
With equation (9) theoretical values of $\rho(0)$ can be calcu-
lated from n and k which can be compared with the respective
experimental values deduced by equation (10) from the reflec-
tivity measurements at $35°$. The experimental values of $\rho(35°)$
are practically identical with $\rho(0°)$ as demonstrated by figure 5.
The best agreement has been obtained between the theoretical
and experimental quantities for the measurements made at 514.5 nm
so that the values of

$$n = 2.0 \qquad \text{and} \qquad k = 0.6$$

represent best preliminary values of the optical constants of
$UO_2$ for the visible spectral range averaged in the temperature
range between 3000 and 3500 K. Considering the scatter in the
measured points of the reflectance curves, the uncertainty
range of n and k can be estimated to be $\pm$ 10% and $\pm$ 40%, respec-
tively.

Figure 5 shows theoretical reflectivity curves calculated from
the equations (5) and (6) for n = 2 and k = 0.6. With these
values of n and k the principle angle of incidence is $\theta_o=65°$
as obtained from equation (7). The bars along the reflectivity
curves for $\rho_p$ and $\rho_s$ which are indicated at the angles of $35°$,
$45°$ and $72°$ represent the reflectivities measured at 3200 K
for $\lambda=514.5$ nm. The lengths of the bars show the experimental
scattering. Figure 6 shows for several values of k the spectral
normal reflectivity $\rho(0)$ calculated from equation (9) as a func-
tion of n. The case of n=2 and k=0.6 is indicated by the dotted
lines; the respective value of $\rho(0)$ is in agreement with our
experimental results for $\rho(0)$.

To desmonstrate the influence of n and k on the course of the
reflectivity curves figure 7 shows theoretical reflectivity cur-
ves vs. the angle of incidence for several pairs of n and k.
With decreasing values of n the principle angle of incidence
is shifted towards smaller angles, whereas with decreasing values
of k the minima of $r_p$ and $r_p/r_s$ are lowered.
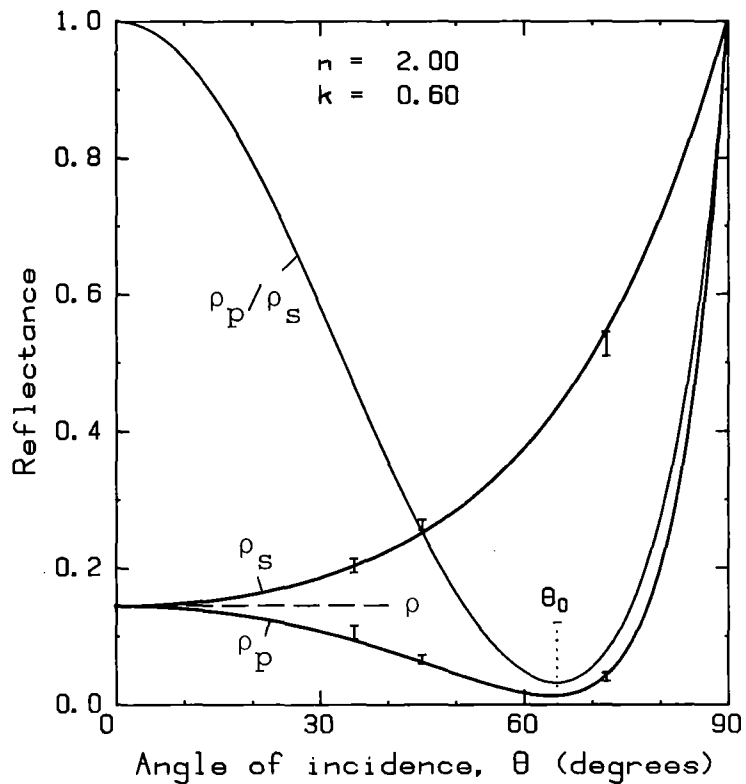
Figure 5: Theoretical reflectivity curves for n=2, k=0.6.
The bars along the curves for $\rho_p$ and $\rho_s$ denote experimental results.
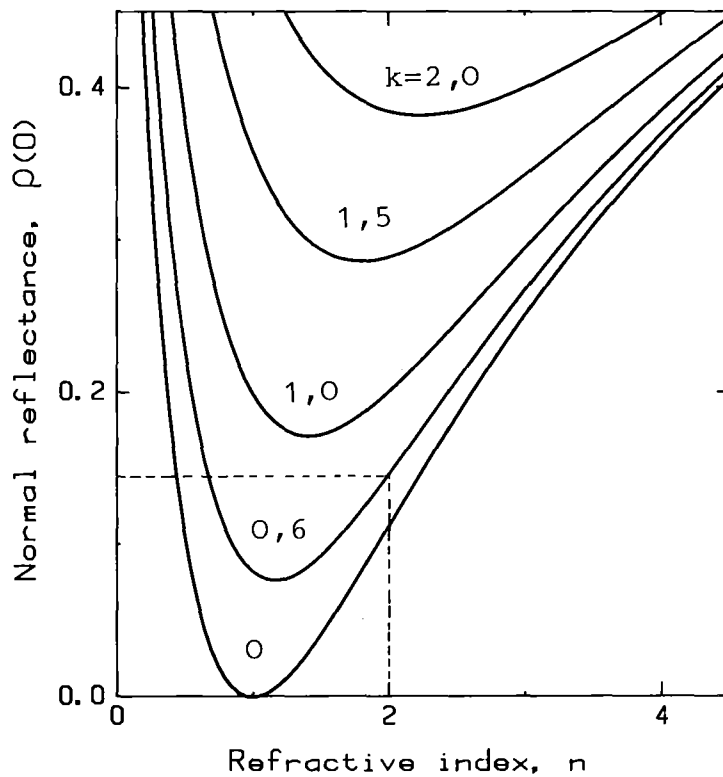


Figure 6: Theoretical normal reflectivity as a function of n; k being the parameter.
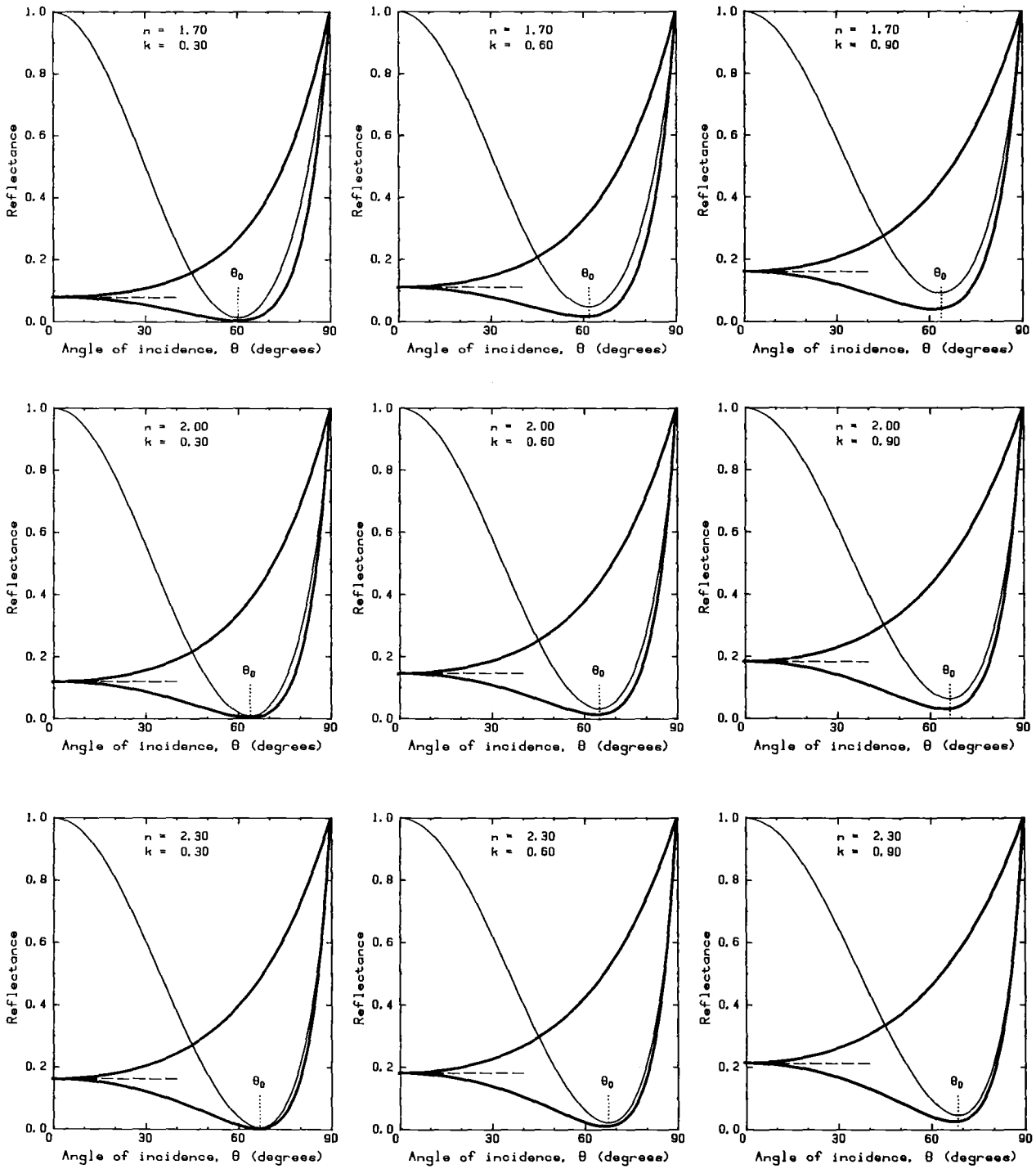
Figure 7: Theoretical reflectivity curves for several pairs of n and k.
(cf. figure 5.)

## 5. Discussion

The scattering of the experimental values shown in figure 3a-i
can be mainly attributed to the imperfections of the reflec-
ting surface and to the spreading of the angle of incidence
caused by the formation of a meniscus in the heated area. With
increasing temperature, oscillations of the liquid surface as
well as vaporization and gas bursts affect the angle of inci-
dence and disturb the smoothness of the surface, which results
in a certain amount of diffuse reflection. This appears from
the check of the measurements at $45^{\circ}$ incidence: Equation (8)
is fulfilled at temperatures up to 3500 K but less well ful-
filled at temperatures above 3500 K. At lower temperatures
recrystallization takes place in the refrozen sample surface
and cracks appear which likewise cause diffuse scattering of
light.

The evaluation of the reflectivity and emissivity of unpolarized
radiation on the basis of equations (1) and (10) turns out to be
little affected by a certain amount of diffuse reflection where-
as the evaluation of the optical constants is limited to tempera-
tures up to 3500 K. To overcome this shortcoming further experi-
ments are planned with dense, single crystal $UO_2$ and by use of
larger heated areas to improve the measurements at a very oblique
incidence.

The results of the reflectivity measurements shown in figures
3a-i are in agreement with previous measurements made at 633 nm
/22/ except for the small discontinuity at the solid-liquid
phase transition observed at 633 nm which could not be clearly
confirmed. The wavelength dependence is similar to that found
by Schoenes /8/ at room temperature but it is less distinct.
An extension of the reflection measurements to longer wavelengths
up to 1060 nm is planned in further experiments.

Figure 4 reveals a deviation of the $UO_2$ emissivity from Lambert's
cosine law shown by the fact that the normal emissivity of $UO_2$
is about 5% higher than its hemispherical emittance. This be-
haviour of $UO_2$ is typical for smooth surfaced ceramics at wave-

lengths of weak absorption /23/. To estimate more reliably
the total thermal emittance of liquid $UO_2$ from its spectral
emittance, the extension of the spectral emissivity measure-
ments to the near infrared is indispensable.

Regarding the evaluation of n and k from reflectivity measure-
ments, the highest sensitivity is reached if the angles of in-
cidence are chosen near the principle angle of incidence. This
appears from the isoreflectance curves for $\rho_p/\rho_n$ shown in
figure 8 for the case of n=2.0 and k=0.6 in the n-k plane at
eight different angles of incidence. For each angle those values
for n and k are plotted which fulfil equation 6 in the ranges
of $1.7 \leq n \leq 2.3$ and $0.3 \leq k \leq 0.9$. Maximum accuracy in evaluation
is obtained if the angles of incidence are chosen such that
the respective isoreflectance curves intersect nearly perpendi-
cularly.

The results obtained for the optical constants of $UO_2$ should
be considered as preliminary values. Although the criteria of
equation (8) and (9) are fairly well satisfied for the averaged
reflectivity curves, the scatter in the measured points causes
a considerable uncertainty in n and k. The sensitivity of n and
k to the errors of the reflectivity measurements depends on the
values of n and k and on the chosen angles of incidence
(cf. figure 7 and 8). For $UO_2$, the accuracy of k in this case
is more influenced than that of n. Further measurements should
include a third intermediate angle near the principal angle of
incidence. With this third angle the measurements could be aver-
aged for n and k and the consistency of the three values of n
and k obtained could serve as a control for the accuracy of the
measurements. A limit of the reflection method is reached when
the reflectivity signal at the critical angle is so small that
the signal-to-noise ratio of the detector prevents accurate
measurements to be made. In the present measurements, this limit
corresponds to values of k of about 0.2 or less.

The values of the refractive index of n=2.0 found for the
molten $UO_2$ is smaller than that of n=2.3 reported by
Ackermann et al. /2/ for room temperature. This reduction
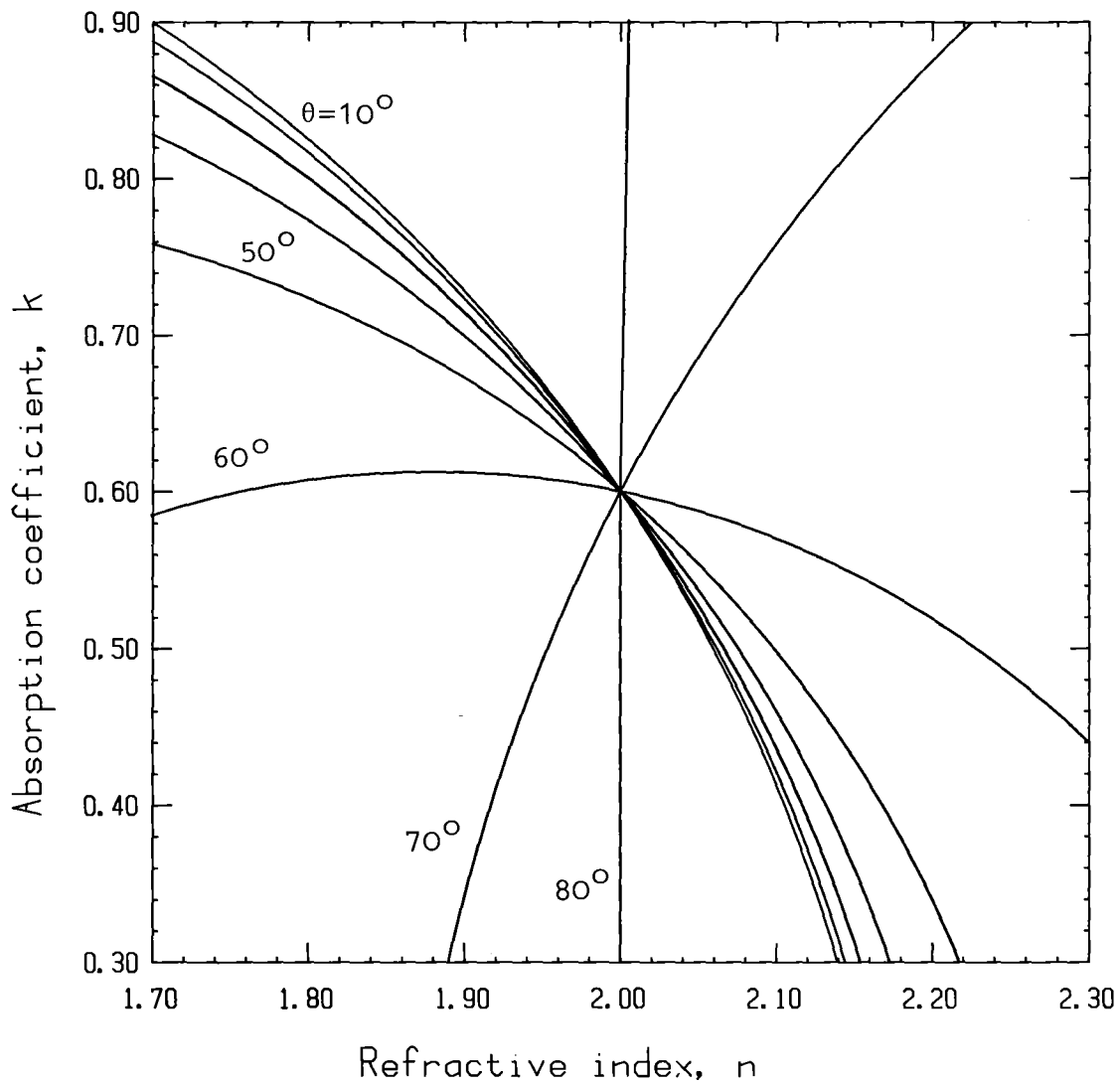
Figure 8: Isoreflectance curves for n=2 and k=0.6 at different angles of incidence

of n could be explained plausibly by assuming a decrease of the electronic polarizability of liquid $UO_2$ / 7/. One additional reflection measurement at room temperature was performed at 647 nm on a smooth-surfaced singly crystal of $UO_2$ which yielded n = 2.25 and confirmed the value of Ackermann /2/.

The preliminary value of k = 0.6 evaluated for the absorption coefficient of liquid $UO_2$ yields an absorption constant of $\alpha \approx 1.5 \cdot 10^5$ cm$^{-1}$ as follows from equation(4). This value of $\alpha$ corresponds to a penetration depth of radiation of about 0.1 µm. Based on this value of $\alpha$, which has been assumed to be valid for the whole visible spectral range up to 700 nm, and on the lower temperature absorption data of single crystal $UO_2$ measured in the near infrared spectral range /4,5/, the contribution of the radiative heat transfer to the thermal conductivity of liquid $UO_2$ was estimated. This estimation shows that the contribution of the radiative heat transfer cannot cause a significant increase of the thermal conductivity of liquid $UO_2$. Based on the result of thermal diffusivity measurements /1/ an increase of the thermal conductivity from ∼0.04 to ∼0.11 Wcm$^{-1}$K$^{-1}$ is expected for $UO_2$ upon melting, but only 10% to 20% of this increase can be explained by radiative heat transfer. At high temperatures near 4000 K the maximum of thermal radiation is shifted towards the visible spectral range. Therefore, with increasing temperature an appreciable augmentation of the internal radiative heat transfer cannot appear because of the high value of $\alpha$ in the visible range.

To substantiate the contribution of the radiative heat transfer to the thermal conductivity of liquid $UO_2$, the preliminary value for the absorption coefficient k and its spectral course must be proved in further experiments. Particularly the course of the absorption coefficient from the visible red towards longer wavelengths is important. At lower temperatures the absorption edge of single crystal $UO_2$ was found near 650 nm /3,8/. An estimate of the absorption edge of liquid $UO_2$ calls for further measurements to be performed at longer wavelengths from 650 nm up to the near infrared.

## Acknowledgement

## References

1. C.S. Kim, R.A. Blomquist, J. Haley, R. Land, J. Fischer,
   M.G. Chasanov, L. Leibowitz,
   in Proceedings of the Seventh Symposium on Thermophysical
   Properties, Ed. A. Cezairliyan (New York: American Society
   of Mechanical Engineers), (1977), pp. 338-343

2. R.J. Ackermann, R.J. Thorn, G.H. Winslow,
   J. Opt. Soc. Am. 49 (1959) 1107-1112

3. J.L. Bates,
   Nucl. Sci. Eng. 21 (1965) 26-29

4. M.J. Davies
   Ph. D. Thesis, University of Leeds, Leeds, England, 1970

5. P. Browning,
   Report AERE-M 3034, Chemistry Division AERE Harwell,
   Oxfordshire, England OX11 ORA (1979)

6. E.E. Anderson,
   Nuclear Technology 30 (1976) 65-70

7. R.A. Young
   J. Nucl. Mater 87 (1979) 283-296

8. J. Schoenes,
   J. Appl. Phys. 49 (1978) 1463-1465

9. F. Cabannes, J.P. Stora, J. Tsakiris,
   C.R. Acad. Sci. Ser. B (1967) 45-48

10. P.C. Held, D.R. Wilder,
    J. Am. Ceram. Soc. 52 (1969) 182-186

11. M. Bober, H.U. Karow, K. Müller,
    High Temperatures - High Pressures 12 (1980)    161-168

12. M. Bober,
    in Proceedings of the Seventh European Thermophysical
    Properties Conference, Antwerpen (Belgium) June 30 - July 4,
    1980, to be published in High Temperatures - High Pressures

13. M. Bober, H.U. Karow,
    in Proceedings of the Seventh Symposium on Thermophysical
    Properties, Ed. A. Cezairliyan (New York: American Society
    of Mechanical Engineers), (1977) pp. 334-350

14. M.N. Özisik,

    "Radiative Transfer", Wiley, New York, 1973

15. E.N. Shestakov, L.N. Latyev, V. Ya.Chekhovskoi,

    High Temperature 16 (1978) 140-151 (Translated from Russian,

    Teplofizika Vysokikh Temperatur 16 (1978) 178-189

16. D. G. Avery,

    Proc. Phys. Soc. B65 (1952) 425-428

17. H.U. Karow,

    Report KfK 2653, Kernforschungszentrum Karlsruhe,

    Federal Republic of Germany, (1979)

18. W.R. Hunter,

    J. Opt. Soc. Am. 55 (1965) 1197-1204

19. M. Born, E. Wolf,

    "Principles of Optics", Pergamon Press, Oxford, 1975

20. H.B. Holl,

    in Proceedings of the Symposium on Thermal Radiation of

    Solids, Ed. S. Katzoff (Washington DC, USA: National

    Aeronautics and Space Administration) Report NASA SP-55

    (1965) pp. 45-61

21. K. Müller,

    Report KfK 2803, Kernforschungszentrum, Karlsruhe,

    Federal Republic of Germany, (1979)

22. H.U. Karow, M. Bober,

    in Proceedings of the IAEA Symposium on Thermodynamics of

    Nuclear Materials, Jülich 1979 (Vienna: IAEA), to be published

23. R.L. Cox,

    in Proceedings of the Symposium on Thermal Radiation of Solids,

    Ed. S. Katzoff (Washington DC. USA: National Aeronautics and

    Space Administration) Report NASA SP-55 (1965) pp. 83-101

Appendix


Table 1a: Measured reflectivities of $UO_2$ for the perpendicular ($\rho_s$) and the parallel ($\rho_p$) components at the wavelength of 647.1 nm and the angle of incidence of 35.5 degrees

| T[K] | $\rho_s$ | T[K] | $\rho_s$ | T[K] | $\rho_p$ | T[K] | $\rho_p$ |
|---|---|---|---|---|---|---|---|
| 3862 | 0.096 | 2914 | 0.196 | 3849 | 0.042 | 2709 | 0.105 |
| 3859 | 0.094 | 2868 | 0.202 | 3823 | 0.044 | 2613 | 0.121 |
| 3855 | 0.117 | 2803 | 0.210 | 3809 | 0.050 | 2507 | 0.096 |
| 3828 | 0.118 | 2792 | 0.201 | 3799 | 0.056 | 2408 | 0.114 |
| 3821 | 0.111 | 2744 | 0.207 | 3794 | 0.055 | 2329 | 0.119 |
| 3773 | 0.131 | 2702 | 0.199 | 3787 | 0.053 | 2301 | 0.104 |
| 3770 | 0.128 | 2671 | 0.216 | 3771 | 0.051 | 2228 | 0.115 |
| 3749 | 0.130 | 2661 | 0.198 | 3760 | 0.063 | 2186 | 0.118 |
| 3744 | 0.125 | 2658 | 0.201 | 3758 | 0.066 | 2163 | 0.111 |
| 3744 | 0.116 | 2572 | 0.202 | 3744 | 0.063 | | |
| 3722 | 0.125 | 2515 | 0.216 | 3734 | 0.063 | | |
| 3718 | 0.157 | 2474 | 0.205 | 3733 | 0.056 | | |
| 3717 | 0.148 | 2375 | 0.201 | 3731 | 0.055 | | |
| 3705 | 0.162 | 2334 | 0.205 | 3731 | 0.072 | | |
| 3703 | 0.162 | 2320 | 0.209 | 3707 | 0.068 | | |
| 3649 | 0.169 | 2296 | 0.203 | 3694 | 0.073 | | |
| 3638 | 0.163 | 2286 | 0.207 | 3685 | 0.078 | | |
| 3637 | 0.165 | 2275 | 0.220 | 3642 | 0.085 | | |
| 3623 | 0.169 | 2264 | 0.215 | 3628 | 0.082 | | |
| 3621 | 0.156 | 2171 | 0.206 | 3614 | 0.083 | | |
| 3579 | 0.163 | 2154 | 0.210 | 3612 | 0.072 | | |
| 3560 | 0.178 | | | 3605 | 0.088 | | |
| 3549 | 0.178 | | | 3569 | 0.077 | | |
| 3540 | 0.189 | | | 3534 | 0.085 | | |
| 3524 | 0.182 | | | 3509 | 0.100 | | |
| 3514 | 0.186 | | | 3502 | 0.087 | | |
| 3495 | 0.173 | | | 3479 | 0.085 | | |
| 3485 | 0.185 | | | 3434 | 0.097 | | |
| 3476 | 0.187 | | | 3420 | 0.096 | | |
| 3447 | 0.203 | | | 3389 | 0.095 | | |
| 3432 | 0.181 | | | 3363 | 0.097 | | |
| 3402 | 0.191 | | | 3294 | 0.107 | | |
| 3380 | 0.179 | | | 3275 | 0.093 | | |
| 3376 | 0.185 | | | 3260 | 0.102 | | |
| 3348 | 0.197 | | | 3224 | 0.096 | | |
| 3329 | 0.197 | | | 3140 | 0.096 | | |
| 3275 | 0.198 | | | 3128 | 0.103 | | |
| 3237 | 0.204 | | | 3112 | 0.092 | | |
| 3117 | 0.215 | | | 3108 | 0.112 | | |
| 3113 | 0.197 | | | 3105 | 0.109 | | |
| 3111 | 0.203 | | | 3083 | 0.120 | | |
| 3106 | 0.208 | | | 3081 | 0.102 | | |
| 3105 | 0.214 | | | 2986 | 0.118 | | |
| 3102 | 0.195 | | | 2943 | 0.103 | | |
| 3099 | 0.191 | | | 2900 | 0.117 | | |
| 3075 | 0.207 | | | 2829 | 0.099 | | |
| 2996 | 0.197 | | | 2807 | 0.111 | | |
| 2970 | 0.213 | | | 2797 | 0.114 | | |
| 2952 | 0.215 | | | 2740 | 0.106 | | |
| 2945 | 0.200 | | | 2721 | 0.116 | | |

Table 1b: Measured reflectivities of $UO_2$ for the perpendicular ($\rho_s$) and the parallel ($\rho_p$) components at the wavelength of 647.1 nm and the angle of incidence of 45.0 degrees

| T[K] | $\rho_s$ | T[K] | $\rho_s$ | T[K] | $\rho_p$ | T[K] | $\rho_p$ |
|---|---|---|---|---|---|---|---|
| 3777 | 0.134 | 2812 | 0.278 x | 3767 | 0.045 | 2469 | 0.087 |
| 3743 | 0.158 | 2770 | 0.269 | 3748 | 0.044 x | 2394 | 0.072 |
| 3740 | 0.163 | 2752 | 0.258 | 3721 | 0.047 | 2394 | 0.085 |
| 3732 | 0.163 x | 2693 | 0.273 | 3695 | 0.047 x | 2269 | 0.087 |
| 3699 | 0.191 | 2663 | 0.273 | 3673 | 0.054 | 2240 | 0.079 |
| 3694 | 0.194 x | 2634 | 0.281 x | 3661 | 0.052 | 2194 | 0.081 |
| 3692 | 0.178 | 2609 | 0.256 x | 3653 | 0.052 x | 2146 | 0.075 x |
| 3690 | 0.171 x | 2591 | 0.269 | 3634 | 0.054 x | 2086 | 0.086 |
| 3689 | 0.184 x | 2551 | 0.273 x | 3633 | 0.054 | | |
| 3683 | 0.182 | 2507 | 0.283 | 3627 | 0.054 | | |
| 3674 | 0.177 | 2502 | 0.254 | 3617 | 0.056 x | | |
| 3649 | 0.197 | 2412 | 0.260 x | 3608 | 0.055 | | |
| 3644 | 0.185 x | 2386 | 0.272 | 3579 | 0.061 | | |
| 3637 | 0.210 x | 2306 | 0.276 | 3579 | 0.057 | | |
| 3632 | 0.197 | 2306 | 0.279 x | 3560 | 0.058 x | | |
| 3619 | 0.196 x | 2269 | 0.258 | 3558 | 0.059 | | |
| 3608 | 0.219 | 2208 | 0.277 | 3557 | 0.059 | | |
| 3593 | 0.205 x | 2171 | 0.259 | 3528 | 0.057 | | |
| 3591 | 0.215 | 2163 | 0.268 | 3525 | 0.060 x | | |
| 3561 | 0.228 x | 2097 | 0.266 x | 3499 | 0.060 x | | |
| 3560 | 0.214 | | | 3472 | 0.062 x | | |
| 3552 | 0.201 | | | 3460 | 0.061 | | |
| 3545 | 0.220 | | | 3443 | 0.063 | | |
| 3519 | 0.228 | | | 3431 | 0.063 | | |
| 3517 | 0.216 x | | | 3398 | 0.062 | | |
| 3510 | 0.224 | | | 3378 | 0.062 | | |
| 3485 | 0.231 | | | 3365 | 0.064 | | |
| 3465 | 0.241 | | | 3360 | 0.067 | | |
| 3457 | 0.223 x | | | 3359 | 0.067 x | | |
| 3457 | 0.236 | | | 3330 | 0.073 | | |
| 3437 | 0.238 | | | 3299 | 0.068 | | |
| 3437 | 0.243 x | | | 3269 | 0.067 | | |
| 3354 | 0.247 | | | 3242 | 0.069 | | |
| 3336 | 0.239 | | | 3205 | 0.068 | | |
| 3310 | 0.248 | | | 3179 | 0.072 | | |
| 3278 | 0.253 | | | 3113 | 0.079 | | |
| 3242 | 0.245 x | | | 3113 | 0.082 | | |
| 3173 | 0.248 | | | 3112 | 0.075 | | |
| 3117 | 0.253 | | | 3103 | 0.071 | | |
| 3115 | 0.248 x | | | 3044 | 0.079 x | | |
| 3111 | 0.256 | | | 2992 | 0.077 | | |
| 3111 | 0.251 x | | | 2876 | 0.081 | | |
| 3107 | 0.257 | | | 2862 | 0.089 | | |
| 3025 | 0.268 | | | 2844 | 0.076 x | | |
| 3017 | 0.245 | | | 2739 | 0.086 | | |
| 2975 | 0.271 x | | | 2736 | 0.077 | | |
| 2957 | 0.264 | | | 2681 | 0.082 | | |
| 2936 | 0.269 | | | 2625 | 0.074 | | |
| 2892 | 0.253 x | | | 2574 | 0.088 | | |
| 2839 | 0.254 | | | 2523 | 0.076 x | | |

x) single crystal $UO_2$

Table 1c: Measured reflectivities of $UO_2$ for the perpendicular ($\rho_s$) and the parallel ($\rho_p$) components at the wavelength of 647.1 nm and the angle of incidence of 72.0 degrees

| T[K] | $\rho_s$ | T[K] | $\rho_p$ |
|---|---|---|---|
| 3816 | 0.263 | 3802 | 0.035 |
| 3798 | 0.231 | 3799 | 0.027 |
| 3761 | 0.311 | 3796 | 0.024 |
| 3754 | 0.281 | 3791 | 0.027 |
| 3747 | 0.302 | 3747 | 0.023 |
| 3741 | 0.279 | 3689 | 0.032 |
| 3694 | 0.339 | 3638 | 0.037 |
| 3686 | 0.358 | 3627 | 0.033 |
| 3671 | 0.394 | 3611 | 0.035 |
| 3656 | 0.356 | 3535 | 0.033 |
| 3644 | 0.374 | 3519 | 0.025 |
| 3644 | 0.370 | 3434 | 0.025 |
| 3572 | 0.366 | 3406 | 0.037 |
| 3560 | 0.401 | 3375 | 0.030 |
| 3541 | 0.456 | 3303 | 0.040 |
| 3514 | 0.441 | 3261 | 0.039 |
| 3513 | 0.454 | 3242 | 0.027 |
| 3457 | 0.457 | 3163 | 0.039 |
| 3427 | 0.450 | 3132 | 0.027 |
| 3251 | 0.479 | 3106 | 0.042 |
| 3217 | 0.471 | 3095 | 0.044 |
| 3214 | 0.489 | 3008 | 0.030 |
| 3205 | 0.458 | 3005 | 0.032 |
| 3200 | 0.458 | 2924 | 0.040 |
| 3140 | 0.495 | 2847 | 0.042 |
| 3112 | 0.492 | 2839 | 0.044 |
| 3108 | 0.469 | 2798 | 0.030 |
| 3103 | 0.484 | 2706 | 0.042 |
| 3101 | 0.482 | 2645 | 0.038 |
| 3015 | 0.497 | 2617 | 0.041 |
| 3011 | 0.465 | 2505 | 0.029 |
| 3010 | 0.500 | 2425 | 0.027 |
| 2944 | 0.483 | 2355 | 0.035 |
| 2913 | 0.489 | 2252 | 0.039 |
| 2816 | 0.481 | 2228 | 0.040 |
| 2778 | 0.471 | 2215 | 0.025 |
| 2768 | 0.486 | 2137 | 0.038 |
| 2747 | 0.512 | | |
| 2710 | 0.474 | | |
| 2578 | 0.485 | | |
| 2558 | 0.497 | | |
| 2422 | 0.484 | | |
| 2405 | 0.482 | | |
| 2386 | 0.508 | | |
| 2301 | 0.474 | | |
| 2280 | 0.518 | | |
| 2179 | 0.487 | | |
| 2118 | 0.480 | | |
| 2097 | 0.502 | | |

Table 1d: Measured reflectivities of $UO_2$ for the perpendicular ($\rho_s$) and the parallel ($\rho_p$) components at the wavelength of 514.5 nm and the angle of incidence of 35.0 degrees

| T[K] | $\rho_s$ | T[K] | $\rho_s$ | T[K] | $\rho_p$ |
|------|----------|------|----------|------|----------|
| 3799 | 0.070 | 2154 | 0.218 | 3822 | 0.051 |
| 3787 | 0.085 |      |          | 3814 | 0.051 |
| 3782 | 0.091 |      |          | 3811 | 0.055 |
| 3759 | 0.117 |      |          | 3802 | 0.053 |
| 3755 | 0.095 |      |          | 3783 | 0.061 |
| 3736 | 0.097 |      |          | 3756 | 0.069 |
| 3734 | 0.096 |      |          | 3754 | 0.060 |
| 3721 | 0.118 |      |          | 3753 | 0.055 |
| 3678 | 0.127 |      |          | 3751 | 0.063 |
| 3671 | 0.134 |      |          | 3711 | 0.072 |
| 3652 | 0.140 |      |          | 3682 | 0.075 |
| 3620 | 0.160 |      |          | 3656 | 0.086 |
| 3610 | 0.161 |      |          | 3621 | 0.087 |
| 3610 | 0.166 |      |          | 3610 | 0.091 |
| 3604 | 0.168 |      |          | 3603 | 0.083 |
| 3544 | 0.166 |      |          | 3578 | 0.089 |
| 3534 | 0.172 |      |          | 3509 | 0.101 |
| 3528 | 0.183 |      |          | 3498 | 0.090 |
| 3422 | 0.193 |      |          | 3495 | 0.093 |
| 3414 | 0.180 |      |          | 3477 | 0.086 |
| 3410 | 0.188 |      |          | 3471 | 0.094 |
| 3308 | 0.199 |      |          | 3387 | 0.105 |
| 3237 | 0.198 |      |          | 3369 | 0.098 |
| 3177 | 0.205 |      |          | 3307 | 0.091 |
| 3167 | 0.192 |      |          | 3260 | 0.097 |
| 3165 | 0.199 |      |          | 3259 | 0.099 |
| 3155 | 0.198 |      |          | 3244 | 0.105 |
| 3119 | 0.207 |      |          | 3146 | 0.103 |
| 3118 | 0.204 |      |          | 3125 | 0.103 |
| 3117 | 0.207 |      |          | 3123 | 0.103 |
| 3115 | 0.210 |      |          | 3121 | 0.102 |
| 3111 | 0.198 |      |          | 3116 | 0.106 |
| 3107 | 0.195 |      |          | 3112 | 0.113 |
| 3088 | 0.217 |      |          | 3112 | 0.095 |
| 3028 | 0.202 |      |          | 3110 | 0.116 |
| 2991 | 0.227 |      |          | 3109 | 0.112 |
| 2913 | 0.198 |      |          | 2982 | 0.115 |
| 2911 | 0.216 |      |          | 2919 | 0.119 |
| 2811 | 0.222 |      |          | 2891 | 0.112 |
| 2691 | 0.213 |      |          | 2797 | 0.117 |
| 2619 | 0.214 |      |          | 2727 | 0.112 |
| 2593 | 0.207 |      |          | 2658 | 0.104 |
| 2556 | 0.232 |      |          | 2585 | 0.119 |
| 2542 | 0.208 |      |          | 2457 | 0.115 |
| 2463 | 0.219 |      |          | 2386 | 0.117 |
| 2408 | 0.216 |      |          | 2351 | 0.119 |
| 2394 | 0.210 |      |          | 2296 | 0.119 |
| 2296 | 0.226 |      |          | 2137 | 0.117 |
| 2240 | 0.210 |      |          |      |          |
| 2215 | 0.223 |      |          |      |          |

Table 1e: Measured reflectivities of $UO_2$ for the perpendicular ($\rho_s$) and the parallel ($\rho_p$) components at the wavelength of 514.5 nm and the angle of incidence of 45.0 degrees

| T[K] | $\rho_s$ | T[K] | $\rho_p$ |
|------|----------|------|----------|
| 3785 | 0.134 | 3764 | 0.043 |
| 3751 | 0.154 | 3751 | 0.042 |
| 3747 | 0.147 | 3703 | 0.051 |
| 3730 | 0.171 | 3686 | 0.047 |
| 3707 | 0.181 | 3642 | 0.050 |
| 3667 | 0.209 | 3606 | 0.058 |
| 3663 | 0.192 | 3576 | 0.053 |
| 3659 | 0.209 | 3553 | 0.044 |
| 3617 | 0.220 | 3526 | 0.057 |
| 3580 | 0.219 | 3523 | 0.054 |
| 3565 | 0.215 | 3518 | 0.053 |
| 3529 | 0.235 | 3466 | 0.072 |
| 3524 | 0.226 | 3422 | 0.058 |
| 3496 | 0.234 | 3398 | 0.061 |
| 3464 | 0.250 | 3359 | 0.066 |
| 3375 | 0.237 | 3168 | 0.063 |
| 3372 | 0.253 | 3148 | 0.069 |
| 3366 | 0.251 | 3120 | 0.067 |
| 3331 | 0.253 | 3118 | 0.059 |
| 3312 | 0.261 | 3115 | 0.069 |
| 3275 | 0.261 | 3114 | 0.070 |
| 3197 | 0.265 | 3040 | 0.063 |
| 3182 | 0.262 | 3020 | 0.070 |
| 3123 | 0.265 | 2904 | 0.074 |
| 3123 | 0.250 | 2843 | 0.074 |
| 3121 | 0.271 | 2747 | 0.073 |
| 3116 | 0.276 | 2634 | 0.071 |
| 3112 | 0.256 | 2591 | 0.073 |
| 3016 | 0.290 | 2563 | 0.066 |
| 2934 | 0.260 | 2530 | 0.081 |
| 2928 | 0.267 | 2463 | 0.074 |
| 2911 | 0.279 | 2398 | 0.074 |
| 2796 | 0.275 | 2311 | 0.075 |
| 2794 | 0.286 | 2179 | 0.066 |
| 2785 | 0.273 | 2127 | 0.074 |
| 2719 | 0.269 | | |
| 2658 | 0.276 | | |
| 2507 | 0.282 | | |
| 2491 | 0.274 | | |
| 2489 | 0.264 | | |
| 2386 | 0.280 | | |
| 2371 | 0.272 | | |
| 2306 | 0.288 | | |
| 2264 | 0.275 | | |
| 2146 | 0.278 | | |
| 2146 | 0.272 | | |

Table 1f: Measured reflectivities of $UO_2$ for the perpendicular ($\rho_s$) and the parallel ($\rho_p$) components at the wavelength of 514.5 nm and the angle of incidence of 72.0 degrees

| T[K] | $\rho_s$ | T[K] | $\rho_s$ | T[K] | $\rho_p$ |
|---|---|---|---|---|---|
| 3789 | 0.223 | 2944 | 0.529 | 3796 | 0.036 |
| 3771 | 0.267 | 2886 | 0.553 | 3736 | 0.037 |
| 3766 | 0.261 | 2883 | 0.531 | 3712 | 0.038 |
| 3756 | 0.273 | 2844 | 0.529 | 3678 | 0.032 |
| 3753 | 0.286 | 2727 | 0.550 | 3665 | 0.042 |
| 3741 | 0.279 | 2725 | 0.542 | 3657 | 0.035 |
| 3733 | 0.267 | 2636 | 0.541 | 3626 | 0.037 |
| 3716 | 0.333 | 2523 | 0.534 | 3602 | 0.036 |
| 3714 | 0.317 | 2502 | 0.559 | 3590 | 0.043 |
| 3708 | 0.330 | 2474 | 0.530 | 3582 | 0.037 |
| 3699 | 0.343 | 2401 | 0.565 | 3535 | 0.038 |
| 3680 | 0.341 | 2375 | 0.537 | 3516 | 0.043 |
| 3671 | 0.373 | 2296 | 0.551 | 3502 | 0.039 |
| 3670 | 0.329 | 2258 | 0.532 | 3463 | 0.039 |
| 3664 | 0.364 | 2246 | 0.537 | 3429 | 0.032 |
| 3641 | 0.417 | 2240 | 0.567 | 3385 | 0.046 |
| 3639 | 0.392 | 2221 | 0.558 | 3323 | 0.044 |
| 3637 | 0.382 | 2075 | 0.564 | 3304 | 0.038 |
| 3627 | 0.371 | 2062 | 0.539 | 3274 | 0.038 |
| 3624 | 0.436 | | | 3246 | 0.044 |
| 3598 | 0.417 | | | 3198 | 0.034 |
| 3590 | 0.414 | | | 3190 | 0.039 |
| 3574 | 0.453 | | | 3112 | 0.051 |
| 3570 | 0.399 | | | 3106 | 0.045 |
| 3561 | 0.448 | | | 3050 | 0.042 |
| 3554 | 0.431 | | | 2981 | 0.043 |
| 3540 | 0.449 | | | 2944 | 0.046 |
| 3540 | 0.455 | | | 2909 | 0.047 |
| 3514 | 0.427 | | | 2857 | 0.040 |
| 3483 | 0.488 | | | 2844 | 0.040 |
| 3433 | 0.476 | | | 2826 | 0.045 |
| 3387 | 0.496 | | | 2806 | 0.048 |
| 3356 | 0.498 | | | 2685 | 0.048 |
| 3349 | 0.510 | | | 2574 | 0.039 |
| 3302 | 0.510 | | | 2542 | 0.042 |
| 3300 | 0.517 | | | 2505 | 0.041 |
| 3298 | 0.525 | | | 2444 | 0.036 |
| 3278 | 0.533 | | | 2418 | 0.043 |
| 3235 | 0.510 | | | 2338 | 0.043 |
| 3207 | 0.511 | | | 2306 | 0.039 |
| 3199 | 0.525 | | | 2246 | 0.045 |
| 3171 | 0.540 | | | 2171 | 0.044 |
| 3113 | 0.523 | | | 2137 | 0.042 |
| 3112 | 0.526 | | | 2108 | 0.047 |
| 3112 | 0.529 | | | | |
| 3109 | 0.509 | | | | |
| 3101 | 0.530 | | | | |
| 3098 | 0.547 | | | | |
| 3025 | 0.539 | | | | |
| 2989 | 0.551 | | | | |

Table 1g: Measured reflectivities of $UO_2$ for the perpendicular ($\rho_s$) and the parallel ($\rho_p$) components at the wavelength of 458.0 nm and the angle of incidence of 35.5 degrees

| T[K] | $\rho_s$ | T[K] | $\rho_s$ | T[K] | $\rho_p$ | T[K] | $\rho_p$ |
|------|----------|------|----------|------|----------|------|----------|
| 3796 | 0.107 | 2701 | 0.233 | 3938 | 0.028 | 2146 | 0.114 |
| 3768 | 0.137 | 2652 | 0.220 | 3844 | 0.058 | | |
| 3747 | 0.124 | 2585 | 0.241 | 3801 | 0.065 | | |
| 3744 | 0.130 | 2561 | 0.233 | 3773 | 0.059 | | |
| 3710 | 0.160 | 2502 | 0.249 | 3761 | 0.070 | | |
| 3705 | 0.141 | 2477 | 0.228 | 3754 | 0.062 | | |
| 3704 | 0.166 | 2472 | 0.232 | 3725 | 0.077 | | |
| 3692 | 0.150 | 2355 | 0.227 | 3703 | 0.075 | | |
| 3641 | 0.172 | 2338 | 0.237 | 3688 | 0.085 | | |
| 3631 | 0.174 | 2221 | 0.243 | 3654 | 0.088 | | |
| 3622 | 0.177 | 2171 | 0.238 | 3648 | 0.082 | | |
| 3603 | 0.173 | 2154 | 0.223 | 3585 | 0.093 | | |
| 3596 | 0.186 | 2086 | 0.235 | 3584 | 0.095 | | |
| 3592 | 0.199 | | | 3538 | 0.092 | | |
| 3581 | 0.179 | | | 3490 | 0.101 | | |
| 3576 | 0.189 | | | 3467 | 0.098 | | |
| 3575 | 0.181 | | | 3459 | 0.103 | | |
| 3549 | 0.195 | | | 3428 | 0.102 | | |
| 3533 | 0.191 | | | 3424 | 0.099 | | |
| 3493 | 0.206 | | | 3416 | 0.103 | | |
| 3465 | 0.200 | | | 3387 | 0.107 | | |
| 3445 | 0.204 | | | 3375 | 0.103 | | |
| 3445 | 0.209 | | | 3353 | 0.104 | | |
| 3420 | 0.205 | | | 3294 | 0.111 | | |
| 3402 | 0.216 | | | 3262 | 0.107 | | |
| 3360 | 0.219 | | | 3255 | 0.108 | | |
| 3335 | 0.219 | | | 3176 | 0.108 | | |
| 3330 | 0.220 | | | 3168 | 0.116 | | |
| 3325 | 0.217 | | | 3108 | 0.112 | | |
| 3305 | 0.212 | | | 3107 | 0.124 | | |
| 3235 | 0.220 | | | 3107 | 0.105 | | |
| 3227 | 0.225 | | | 3103 | 0.113 | | |
| 3195 | 0.223 | | | 3099 | 0.112 | | |
| 3129 | 0.228 | | | 3019 | 0.119 | | |
| 3116 | 0.219 | | | 2999 | 0.129 | | |
| 3109 | 0.221 | | | 2960 | 0.117 | | |
| 3108 | 0.224 | | | 2918 | 0.112 | | |
| 3105 | 0.233 | | | 2846 | 0.121 | | |
| 3105 | 0.224 | | | 2770 | 0.113 | | |
| 3097 | 0.218 | | | 2752 | 0.116 | | |
| 3021 | 0.235 | | | 2743 | 0.119 | | |
| 3016 | 0.234 | | | 2665 | 0.120 | | |
| 2981 | 0.228 | | | 2556 | 0.126 | | |
| 2954 | 0.235 | | | 2540 | 0.120 | | |
| 2875 | 0.250 | | | 2441 | 0.117 | | |
| 2873 | 0.234 | | | 2363 | 0.113 | | |
| 2843 | 0.226 | | | 2351 | 0.121 | | |
| 2824 | 0.233 | | | 2258 | 0.113 | | |
| 2824 | 0.234 | | | 2252 | 0.134 | | |
| 2731 | 0.227 | | | 2154 | 0.118 | | |

Table 1h: Measured reflectivities  of $UO_2$ for  the perpendicular ($\rho_s$) and the parallel ($\rho_p$) components at  the wavelength of 458.0 nm and  the angle of  incidence of 46.0 degrees

| T[K] | $\rho_s$ | T[K] | $\rho_s$ | T[K] | $\rho_p$ | T[K] | $\rho_p$ |
|------|------|------|------|------|------|------|------|
| 3832 | 0.138 | 3028 | 0.268 | 3883 | 0.019 | 2505 | 0.085 |
| 3812 | 0.149 | 3015 | 0.291 | 3855 | 0.032 | 2469 | 0.080 |
| 3804 | 0.156 | 3015 | 0.288 | 3851 | 0.031 | 2401 | 0.076 |
| 3803 | 0.164 | 2966 | 0.283 | 3824 | 0.033 | 2363 | 0.089 |
| 3771 | 0.165 | 2904 | 0.274 | 3649 | 0.059 | 2311 | 0.086 |
| 3761 | 0.175 | 2900 | 0.283 | 3613 | 0.061 | 2228 | 0.075 |
| 3748 | 0.175 | 2872 | 0.283 | 3579 | 0.065 | 2201 | 0.089 |
| 3737 | 0.174 | 2807 | 0.281 | 3576 | 0.065 | 2097 | 0.072 |
| 3733 | 0.191 | 2792 | 0.271 | 3533 | 0.065 | | |
| 3713 | 0.193 | 2783 | 0.296 | 3522 | 0.054 | | |
| 3674 | 0.222 | 2724 | 0.288 | 3500 | 0.067 | | |
| 3668 | 0.194 | 2593 | 0.297 | 3481 | 0.058 | | |
| 3667 | 0.198 | 2593 | 0.283 | 3462 | 0.058 | | |
| 3628 | 0.220 | 2563 | 0.268 | 3462 | 0.063 | | |
| 3624 | 0.211 | 2530 | 0.297 | 3442 | 0.067 | | |
| 3621 | 0.234 | 2489 | 0.268 | 3427 | 0.063 | | |
| 3577 | 0.235 | 2463 | 0.272 | 3396 | 0.071 | | |
| 3569 | 0.232 | 2363 | 0.296 | 3372 | 0.071 | | |
| 3563 | 0.230 | 2351 | 0.285 | 3337 | 0.071 | | |
| 3551 | 0.244 | 2315 | 0.275 | 3291 | 0.069 | | |
| 3547 | 0.226 | 2163 | 0.286 | 3281 | 0.067 | | |
| 3543 | 0.252 | 2154 | 0.290 | 3279 | 0.066 | | |
| 3533 | 0.253 | 2062 | 0.278 | 3230 | 0.074 | | |
| 3527 | 0.243 | | | 3223 | 0.069 | | |
| 3521 | 0.258 | | | 3216 | 0.070 | | |
| 3503 | 0.247 | | | 3198 | 0.074 | | |
| 3483 | 0.243 | | | 3170 | 0.078 | | |
| 3475 | 0.253 | | | 3159 | 0.071 | | |
| 3467 | 0.252 | | | 3113 | 0.086 | | |
| 3448 | 0.259 | | | 3109 | 0.078 | | |
| 3442 | 0.253 | | | 3109 | 0.079 | | |
| 3418 | 0.262 | | | 3107 | 0.075 | | |
| 3408 | 0.259 | | | 3021 | 0.082 | | |
| 3408 | 0.261 | | | 3000 | 0.092 | | |
| 3352 | 0.269 | | | 2987 | 0.073 | | |
| 3338 | 0.270 | | | 2966 | 0.089 | | |
| 3331 | 0.250 | | | 2924 | 0.091 | | |
| 3322 | 0.274 | | | 2907 | 0.075 | | |
| 3307 | 0.270 | | | 2888 | 0.085 | | |
| 3301 | 0.269 | | | 2861 | 0.074 | | |
| 3215 | 0.275 | | | 2807 | 0.083 | | |
| 3162 | 0.258 | | | 2768 | 0.081 | | |
| 3162 | 0.283 | | | 2759 | 0.073 | | |
| 3119 | 0.283 | | | 2725 | 0.076 | | |
| 3114 | 0.273 | | | 2716 | 0.085 | | |
| 3111 | 0.256 | | | 2649 | 0.089 | | |
| 3110 | 0.266 | | | 2632 | 0.085 | | |
| 3107 | 0.278 | | | 2595 | 0.077 | | |
| 3107 | 0.273 | | | 2576 | 0.088 | | |
| 3106 | 0.276 | | | 2549 | 0.076 | | |

Table 1i: Measured reflectivities of $UO_2$ for the perpendicular ($\rho_s$) and the parallel ($\rho_p$) components at the wavelength of 458.0 nm and the angle of incidence of 73.0 degrees

| T[K] | $\rho_s$ | T[K] | $\rho_p$ |
|------|----------|------|----------|
| 3798 | 0.212 | 3786 | 0.048 |
| 3767 | 0.237 | 3770 | 0.057 |
| 3764 | 0.225 | 3764 | 0.048 |
| 3764 | 0.204 | 3744 | 0.051 |
| 3762 | 0.206 | 3704 | 0.054 |
| 3735 | 0.292 | 3701 | 0.051 |
| 3731 | 0.220 | 3696 | 0.042 |
| 3701 | 0.278 | 3644 | 0.057 |
| 3699 | 0.264 | 3633 | 0.055 |
| 3690 | 0.339 | 3615 | 0.046 |
| 3689 | 0.347 | 3579 | 0.063 |
| 3684 | 0.309 | 3533 | 0.063 |
| 3651 | 0.314 | 3526 | 0.060 |
| 3615 | 0.382 | 3511 | 0.053 |
| 3608 | 0.368 | 3504 | 0.054 |
| 3595 | 0.421 | 3489 | 0.068 |
| 3539 | 0.371 | 3460 | 0.052 |
| 3512 | 0.431 | 3413 | 0.069 |
| 3505 | 0.453 | 3384 | 0.055 |
| 3467 | 0.452 | 3318 | 0.055 |
| 3464 | 0.454 | 3190 | 0.058 |
| 3429 | 0.460 | 3126 | 0.059 |
| 3393 | 0.479 | 3111 | 0.064 |
| 3377 | 0.473 | 3105 | 0.083 |
| 3297 | 0.483 | 3098 | 0.068 |
| 3246 | 0.499 | 3098 | 0.064 |
| 3162 | 0.499 | 3091 | 0.074 |
| 3115 | 0.506 | 3028 | 0.065 |
| 2972 | 0.535 | 2980 | 0.074 |
| 2965 | 0.516 | 2958 | 0.061 |
| 2909 | 0.496 | 2876 | 0.075 |
| 2868 | 0.536 | 2797 | 0.064 |
| 2844 | 0.508 | 2671 | 0.068 |
| 2754 | 0.514 | 2615 | 0.068 |
| 2740 | 0.540 | 2542 | 0.065 |
| 2630 | 0.498 | 2375 | 0.071 |
| 2613 | 0.516 | 2355 | 0.062 |
| 2578 | 0.541 | 2351 | 0.066 |
| 2480 | 0.513 | 2269 | 0.071 |
| 2448 | 0.544 | 2208 | 0.068 |
| 2405 | 0.521 | | |
| 2325 | 0.517 | | |
| 2269 | 0.498 | | |
| 2258 | 0.541 | | |
| 2240 | 0.530 | | |
| 2163 | 0.535 | | |
| 2118 | 0.508 | | |

Table 2a: Reflectivity of $UO_2$ at the wavelength of 647 nm averaged at different temperatures for three angles of incidence

| T [K] | $\theta^0$ | $\rho_s$ | $\rho_p$ | $\rho_p/\rho_s$ | $\rho$ |
|-------|-----------|----------|----------|-----------------|--------|
| 2500  | 35.5      | 0.206    | 0.111    | 0.539           | 0.159  |
|       | 45.0      | 0.268    | 0.078    | 0.291           | 0.173  |
|       | 72.0      | 0.489    | 0.035    | 0.072           | 0.262  |
| 2800  | 35.5      | 0.205    | 0.110    | 0.537           | 0.158  |
|       | 45.0      | 0.266    | 0.078    | 0.293           | 0.172  |
|       | 72.0      | 0.488    | 0.035    | 0.072           | 0.262  |
| 3000  | 35.5      | 0.204    | 0.109    | 0.534           | 0.156  |
|       | 45.0      | 0.262    | 0.075    | 0.286           | 0.169  |
|       | 72.0      | 0.486    | 0.035    | 0.072           | 0.260  |
| 3200  | 35.5      | 0.200    | 0.105    | 0.525           | 0.152  |
|       | 45.0      | 0.255    | 0.071    | 0.278           | 0.163  |
|       | 72.0      | 0.480    | 0.034    | 0.071           | 0.257  |
| 3500  | 35.5      | 0.184    | 0.091    | 0.495           | 0.138  |
|       | 45.0      | 0.230    | 0.060    | 0.261           | 0.145  |
|       | 72.0      | 0.437    | 0.032    | 0.073           | 0.235  |
| 3700  | 35.5      | 0.151    | 0.069    | 0.457           | 0.110  |
|       | 45.0      | 0.180    | 0.047    | 0.261           | 0.113  |
|       | 72.0      | 0.344    | 0.028    | 0.081           | 0.186  |

Table 2b: Reflectivity of $UO_2$ at the wavelength of 514.5 nm averaged at different temperatures for three angles of incidence.

| T [K] | $\theta^0$ | $\rho_s$ | $\rho_p$ | $\rho_p/\rho_s$ | $\rho$ |
|-------|-----------|----------|----------|-----------------|--------|
| 2500 | 35.0 | 0.215 | 0.113 | 0.526 | 0.164 |
|      | 45.0 | 0.274 | 0.074 | 0.270 | 0.174 |
|      | 72.0 | 0.547 | 0.041 | 0.075 | 0.294 |
| 2800 | 35.0 | 0.213 | 0.112 | 0.526 | 0.163 |
|      | 45.0 | 0.272 | 0.072 | 0.265 | 0.172 |
|      | 72.0 | 0.545 | 0.041 | 0.075 | 0.293 |
| 3000 | 35.0 | 0.210 | 0.109 | 0.519 | 0.160 |
|      | 45.0 | 0.270 | 0.071 | 0.263 | 0.170 |
|      | 72.0 | 0.538 | 0.041 | 0.076 | 0.289 |
| 3200 | 35.0 | 0.203 | 0.105 | 0.517 | 0.154 |
|      | 45.0 | 0.263 | 0.066 | 0.251 | 0.164 |
|      | 72.0 | 0.527 | 0.040 | 0.076 | 0.283 |
| 3500 | 35.0 | 0.181 | 0.094 | 0.519 | 0.138 |
|      | 45.0 | 0.238 | 0.057 | 0.239 | 0.147 |
|      | 72.0 | 0.465 | 0.037 | 0.080 | 0.251 |
| 3700 | 35.0 | 0.131 | 0.074 | 0.565 | 0.103 |
|      | 45.0 | 0.182 | 0.045 | 0.247 | 0.114 |
|      | 72.0 | 0.336 | 0.034 | 0.101 | 0.185 |

Table 2c: Reflectivity of $UO_2$ at the wavelength of 485 nm averaged at different temperatures for three angles of incidence.

| T $|K|$ | $\theta^0$ | $\rho_s$ | $\rho_p$ | $\rho_p/\rho_s$ | $\rho$ |
|---|---|---|---|---|---|
| 2500 | 35.5 | 0.234 | 0.117 | 0.500 | 0.176 |
| | 46.0 | 0.283 | 0.081 | 0.286 | 0.182 |
| | 73.0 | 0.524 | 0.066 | 0.126 | 0.295 |
| 2800 | 35.5 | 0.233 | 0.116 | 0.498 | 0.175 |
| | 46.0 | 0.282 | 0.080 | 0.284 | 0.181 |
| | 73.0 | 0.522 | 0.066 | 0.126 | 0.294 |
| 3000 | 35.5 | 0.229 | 0.114 | 0.498 | 0.172 |
| | 46.0 | 0.280 | 0.077 | 0.275 | 0.179 |
| | 73.0 | 0.515 | 0.065 | 0.126 | 0.290 |
| 3200 | 35.5 | 0.224 | 0.110 | 0.491 | 0.167 |
| | 46.0 | 0.275 | 0.074 | 0.269 | 0.174 |
| | 73.0 | 0.502 | 0.063 | 0.125 | 0.282 |
| 3500 | 35.5 | 0.199 | 0.098 | 0.492 | 0.148 |
| | 46.0 | 0.248 | 0.062 | 0.250 | 0.155 |
| | 73.0 | 0.443 | 0.058 | 0.131 | 0.250 |
| 3700 | 35.5 | 0.155 | 0.077 | 0.497 | 0.116 |
| | 46.0 | 0.199 | 0.046 | 0.231 | 0.123 |
| | 73.0 | 0.310 | 0.051 | 0.165 | 0.180 |

Table 3: Spectral near-normal $(\varepsilon^n)$ and hemispherical $(\varepsilon^h)$ emissivity of $UO_2$ at three wavelengths $\lambda$.

| T (K) | $\lambda = 647$ nm | | $\lambda = 514.5$ nm | | $\lambda = 458$ nm | |
|-------|-----------|-----------|-----------|-----------|-----------|-----------|
|       | $\varepsilon^n$ | $\varepsilon^h$ | $\varepsilon^n$ | $\varepsilon^h$ | $\varepsilon^n$ | $\varepsilon^h$ |
| 2500  | 0.842 | 0.801 | 0.836 | 0.792 | 0.825 | 0.791 |
| 2800  | 0.845 | 0.805 | 0.838 | 0.792 | 0.826 | 0.790 |
| 3000  | 0.849 | 0.807 | 0.841 | 0.794 | 0.829 | 0.791 |
| 3200  | 0.855 | 0.810 | 0.846 | 0.811 | 0.833 | 0.794 |
| 3500  | 0.871 | 0.830 | 0.863 | 0.819 | 0.852 | 0.817 |
| 3700  | 0.891 | 0.858 | 0.898 | 0.875 | 0.884 | 0.859 |
| 3800  | 0.910 | 0.888 | 0.934 | 0.901 | 0.912 | 0.890 |

Table 4: Spectral near-normal $(\varepsilon^n)$ and hemispherical $(\varepsilon^h)$ emittance of $UO_2$ averaged over the wavelength interval $\Delta\lambda$ (458 nm, 647 nm)

| T (K) | $\varepsilon^n$ | $\varepsilon^h$ |
|-------|-----------|-----------|
| 2500  | 0.838 | 0.797 |
| 2800  | 0.841 | 0.799 |
| 3000  | 0.844 | 0.800 |
| 3200  | 0.849 | 0.813 |
| 3500  | 0.865 | 0.823 |
| 3700  | 0.894 | 0.866 |
| 3800  | 0.922 | 0.895 |